

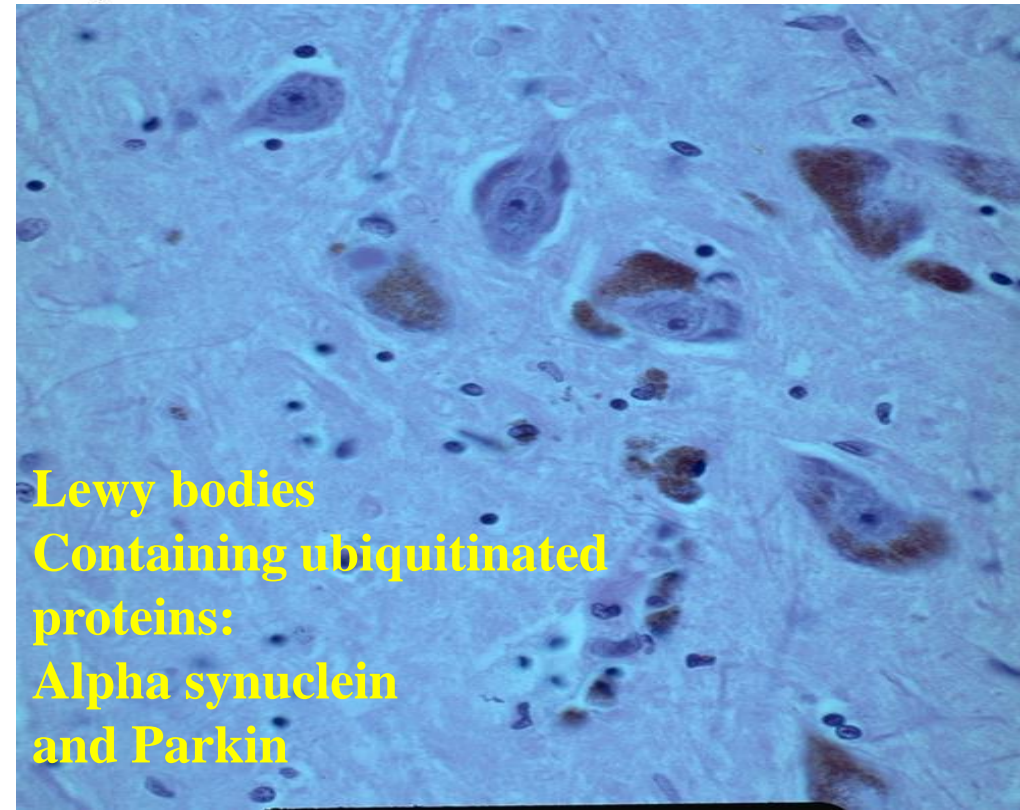
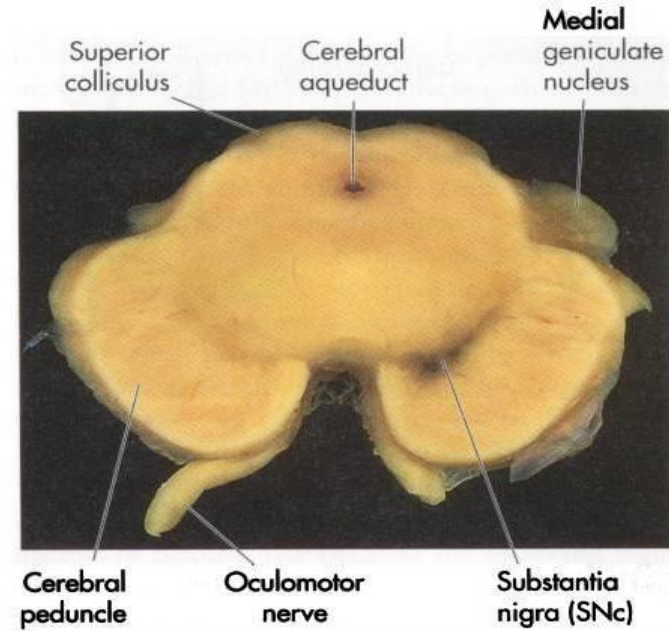
Lecture 6

Regenerative Medicine –
replacement of dopamine producing
cells for Parkinson Disease

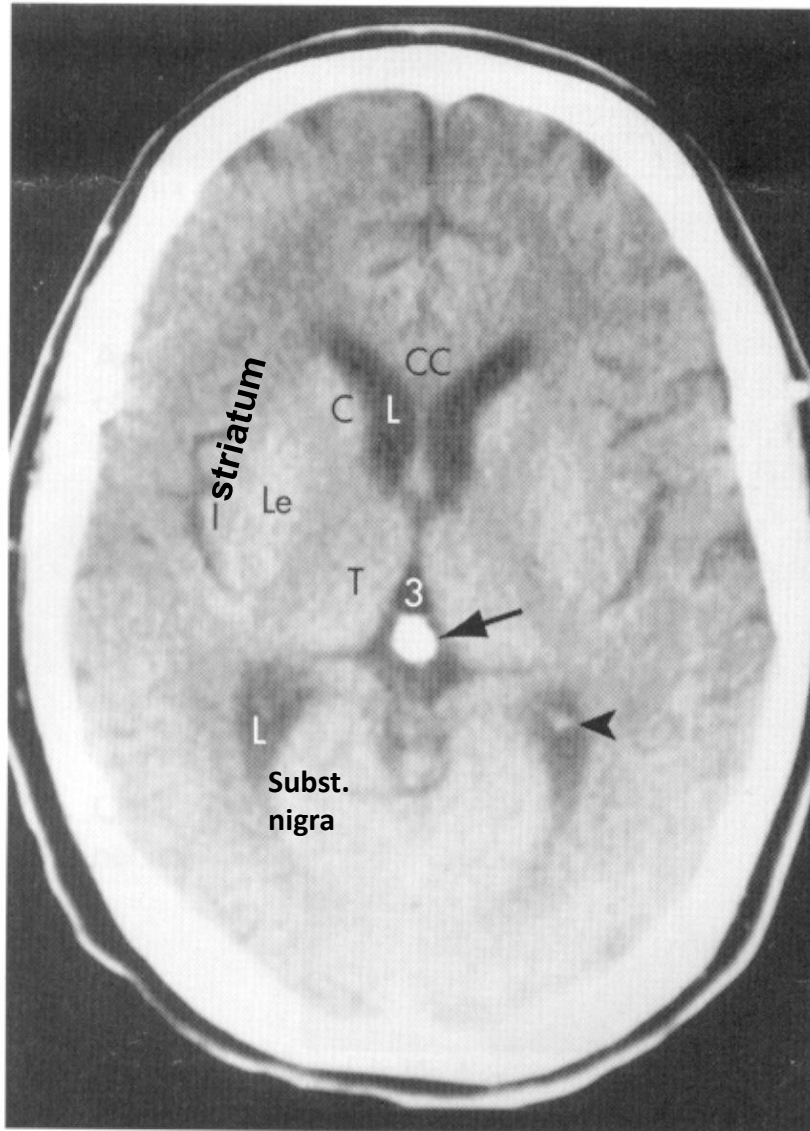
Parkinson Disease is associated with a loss of DA neurons in SNc



- bradykinesia- (slow) and hypokinesia (few movements); resting tremors rigidity - coactivation of flexors and extensors, dystonia (selected muscle group),



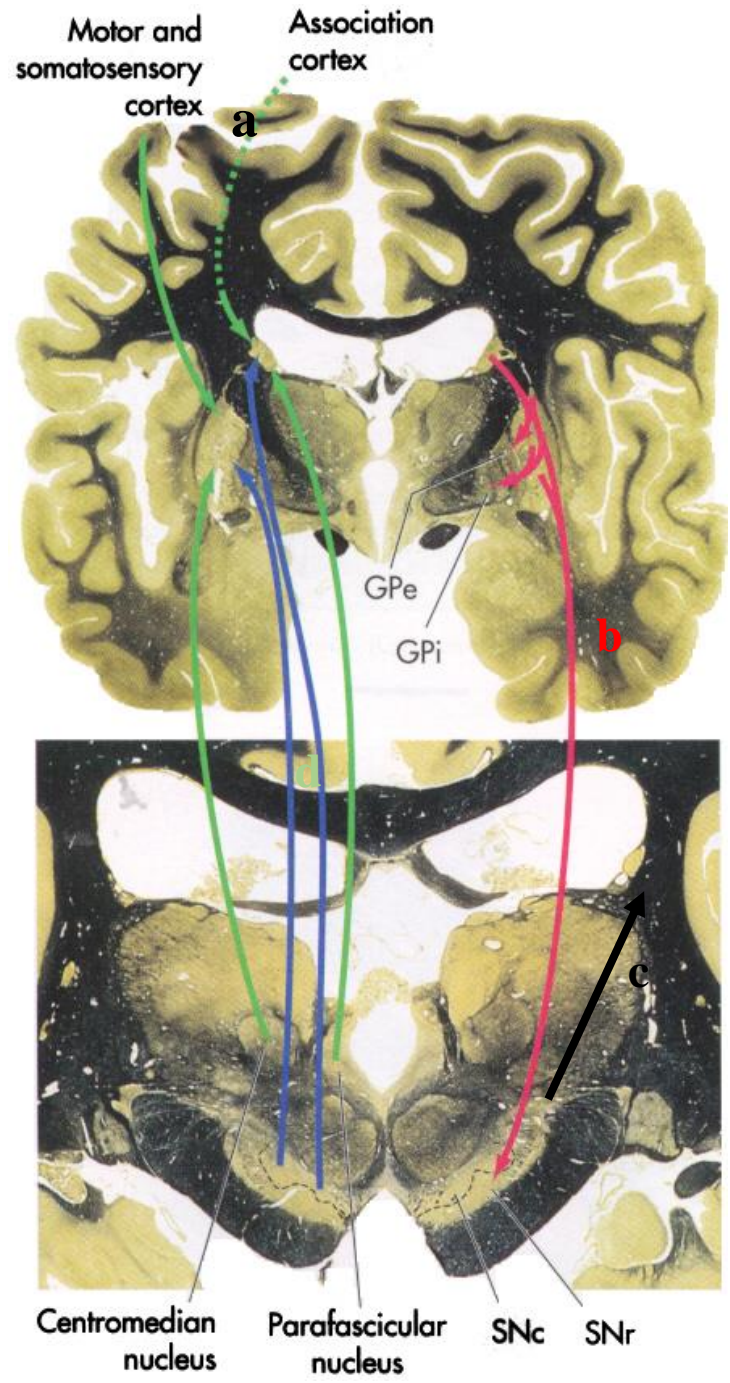
**Lewy bodies
Containing ubiquitinated
proteins:
Alpha synuclein
and Parkin**



Basal Ganglia connected by Dopamine neurons:
telencepalon (striatum = caudate + putamen)

Midbrain (substantia nigra pars compacta)

FIGURE 16-4
Uncontrasted CT of a normal 58-year-old-man. Calcium deposits in the pineal gland (*arrow*) and in the glomus (enlarged region of



(d) Nigro (SNc)-striatal_{DA} projection

Striatum= caudate nucleus + putamen

Substantia nigra

Etiology of Parkinson's Disease (PD) – primarily sporadic

Rare Familial forms of PD are caused by mutations in at least three genes:

Hardy "Genetics of Parkinsonism" Movement Disorders 17, 2002, 645-656.

- a. **Autosomal-recessive juvenile parkinsonism (ARJP)** (*Kitada 1988, Nature 392, 605-8*)
(6q25.2-q27) – mutations of gene encoding Parkin protein.

**Parkin (51kDa): Ring-zinc finger protein, has protein-ubiquitin ligase activity
(ubiquitin carboxy-terminal hydrolase (UCHpL1) – a role in protein degradation)**

Present in Lewy bodies.

Transgenic (KO) mice?

- b. **Autosomal-dominant Alpha-synuclein mutation-Lewy body parkinsonism:**

Alpha-synuclein present in Lewy bodies.

A53T mutation (Italian kindred); A30P (German kindred) (Chr.4).

(alpha-SYNC -synaptic function, plasticity?; oligomerizes, fibrillar aggregates);

KO –weak effect> PD; Drosophila expressing alphaSYNC mutants > neurodegeneration).

- c. **Leucine-rich repeat kinase 2 (LRRK2, phosphorylates peroxyredoxin) mutations associated with both familial and sporadic cases of PD. KO – progressive PD**

Positively regulates autophagy through a calcium-dependent activation of the CaMKK/AMPK signaling pathway, increase in lysosomal pH, and calcium release from lysosomes. plays a role in the retrograde trafficking pathway for recycling proteins

between lysosomes and the Golgi apparatus. Regulates neuronal process morphology in the intact central nervous system (CNS).

Plays a role in synaptic vesicle trafficking. May play a role in the phosphorylation of proteins central to Parkinson disease.

- d. Basic Fibroblast Growth Factor (FGF-2) depletion found in all PD patients (genetic) Polymorphism of FGF20 correlates with PD**

Sporadic (nonfamilial) PD (majority of cases):

- e. Inflammation** – injection of bacterial toxin (LPS)
- f. environmental toxins**
- g. Catecholamine metabolites**
- h. Environmental + genetic factors?**

Reviews on mechanisms of PD:

- 1.Zhang et al., Neurobiol. of Disease 7, 240-250 (2000)*
- 2.Annales New York Acad. Sci. (1999) – series on Synuclein*

Loss of basic fibroblast growth factor in substantia nigra neurons in Parkinson's disease

I. Tooyama, MD, PhD; T. Kawamata, MD, PhD; D. Walker, PhD; T. Yamada, MD, PhD; K. Hanai, PhD;
H. Kimura, MD, PhD; M. Iwane, PhD; K. Igarashi, PhD; E.G. McGeer, PhD;
and P.L. McGeer, MD, PhD, FRCP(C)

Neurology 43, 1993, 372-376

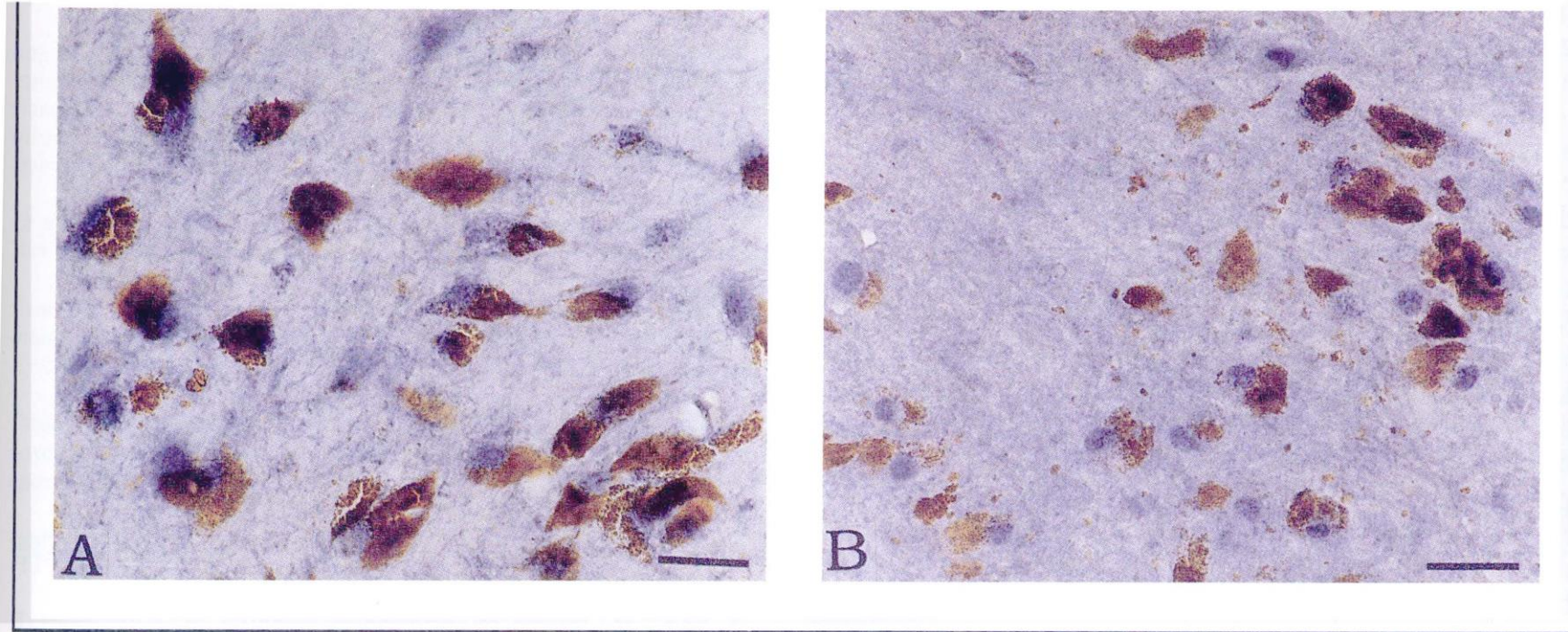


Figure 3. Immunohistochemical staining of nearby sections of a parkinsonian case for TH (A) and bFGF (B). TH-immunoreactivity is present in remaining pigmented cells and processes (A), but only a few bFGF-positive fibers can be seen. Bars = 50 μ m.

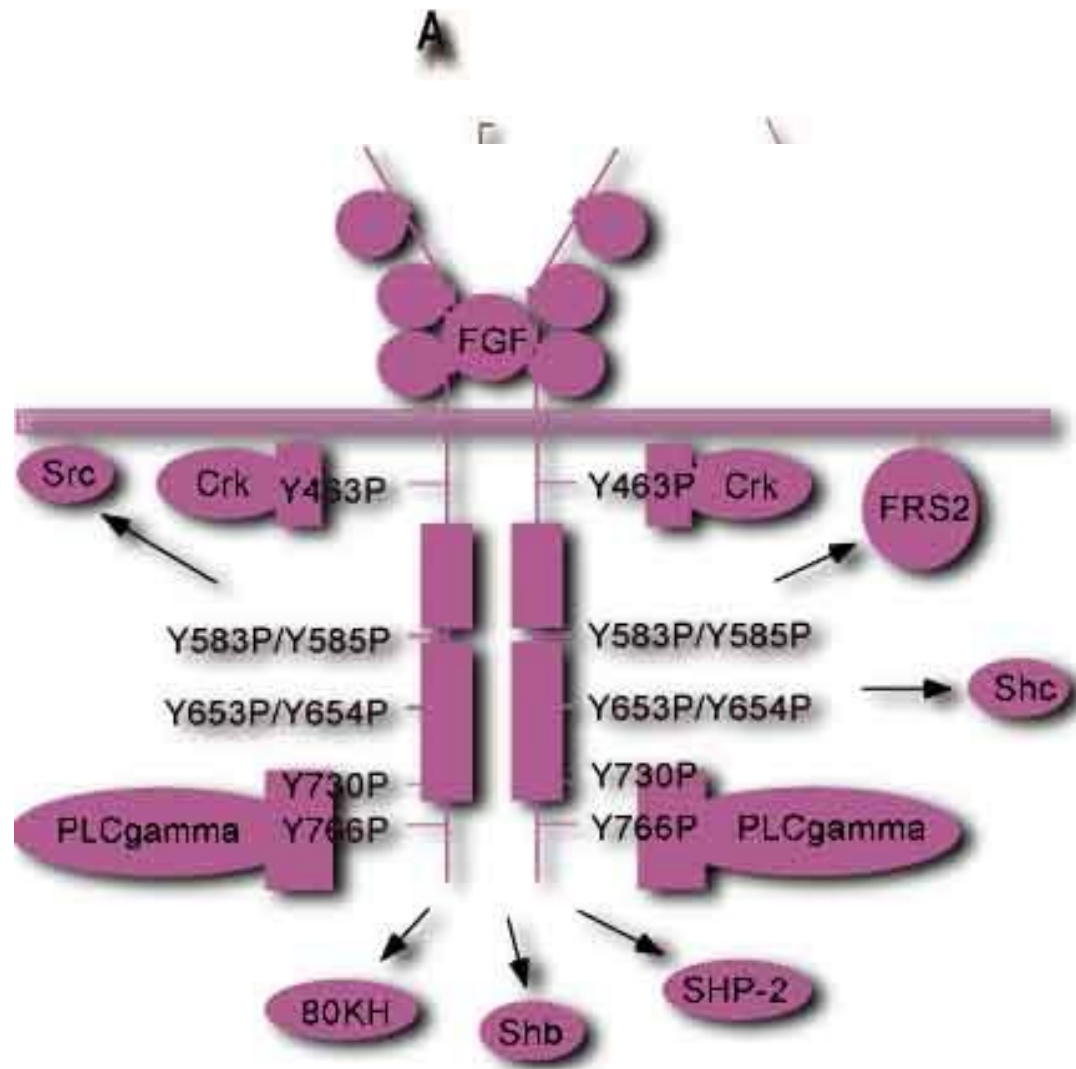
Nearly all melanine+
Are TH+

Only few melanine+
Are FGF-2+

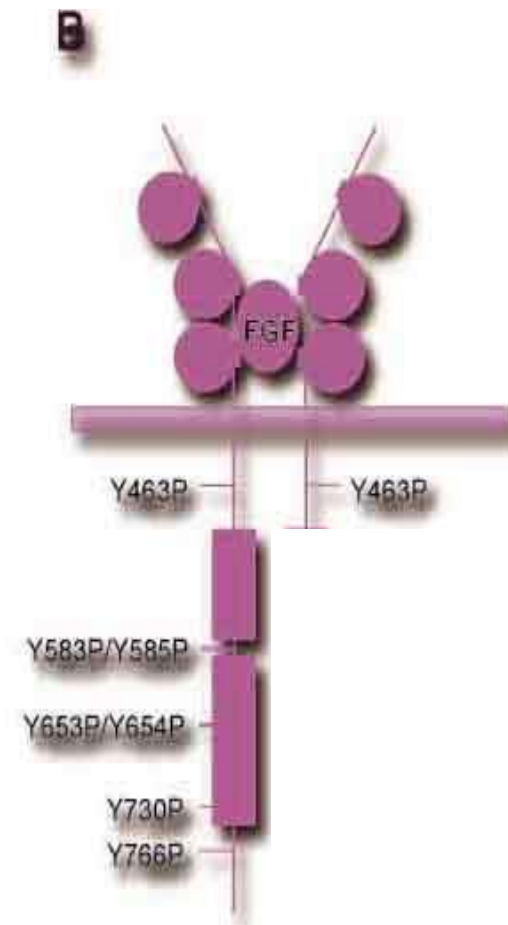
Loss of basic fibroblast growth factor in substantia nigra neurons in Parkinson's disease

I. Tooyama, MD, PhD; T. Kawamata, MD, PhD; D. Walker, PhD; T. Yamada, MD, PhD; K. Hanai, PhD; H. Kimura, MD, PhD; M. Inoue, PhD; B. D. K. Garashi, PhD; E.G. McGeer, PhD; and P.L. McGeer, MD, PhD, FRCP(C)

Type of Neuron	Control	Parkinson	Percent	p value
bFGF* total	1,408 ± 45.2	66 ± 14.6	4.69%	0.0001
pigmented total	1,328 ± 76.6	403 ± 8.7	30.35%	0.0001
bFGF, pigmented	1,275 ± 70.4	33 ± 11.5	2.65%	0.0001
bFGF, nonpigmented	163 ± 34.9	33 ± 7.8	20.25%	0.004
pigmented, non-bFGF	83 ± 16.4	370 ± 18.0	445.8%	0.0001
bFGF, pigmented/ pigmented total	0.937	0.082		



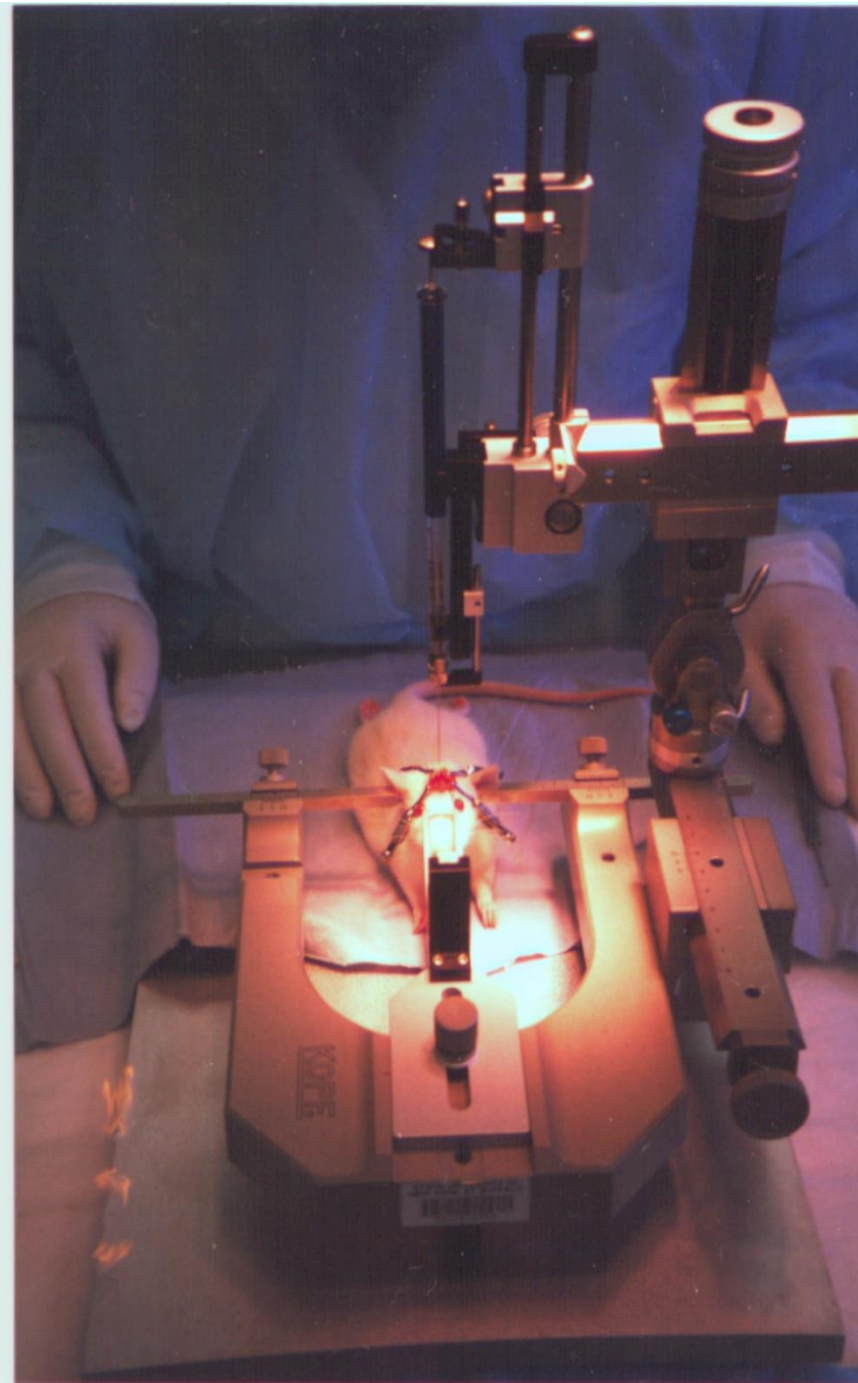
FGFR1



FGFR1(TK-)

Inhibition of FGFR signaling by its dominant negative mutant FGFR1(TK-)

**Stereotaxic
apparatus
for rats
intracerebral
injections**



FGFR1(TK-)

Beta-Gal

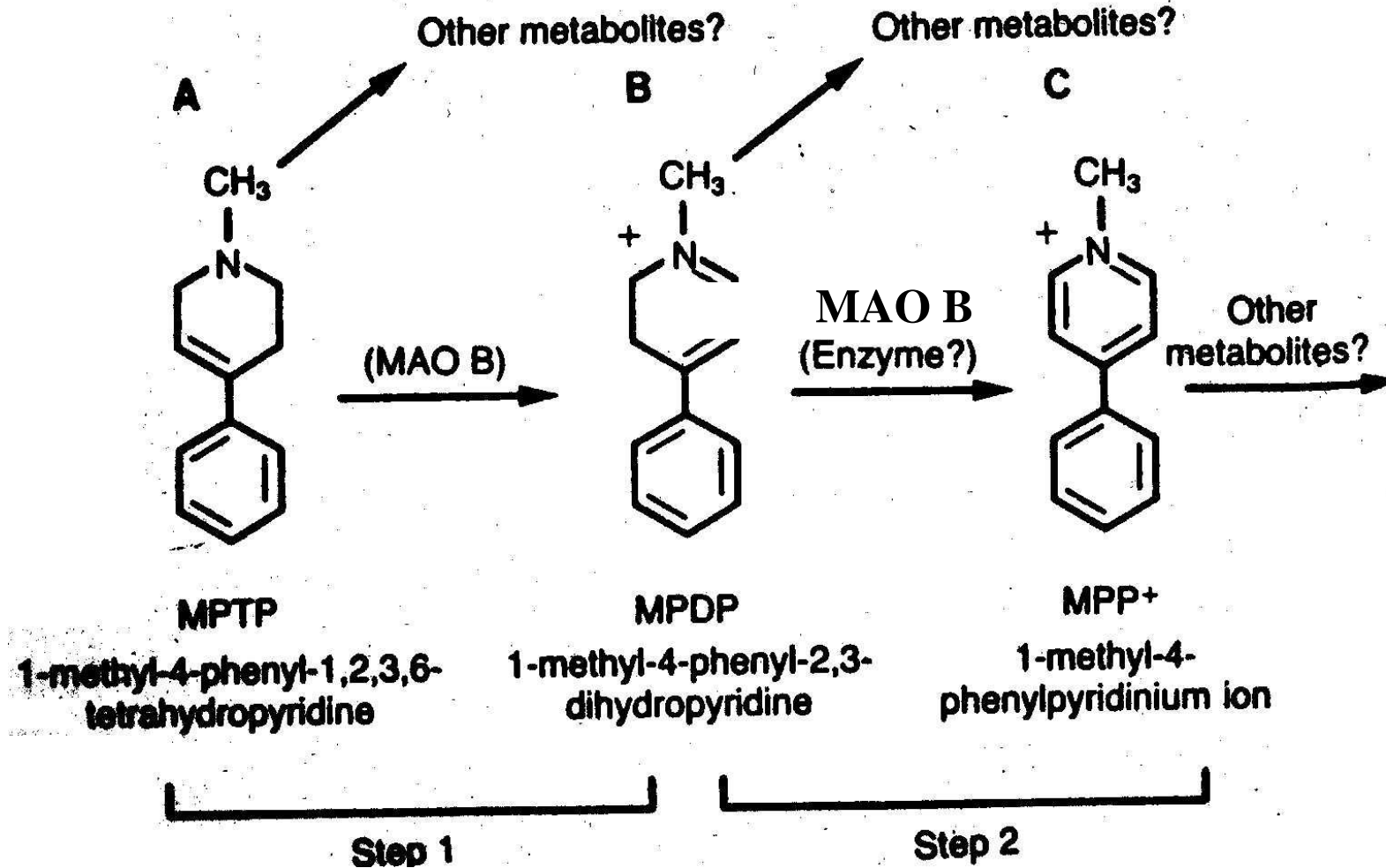
Molecular Brain Research vol. 139, pp 361-366 (2005)

Environmental Hypothesis

The Frozen Addicts



MPTP a contaminating product of meperidine (synthetic heroine) is oxidized by Monoamine Oxidase to highly toxic MPP+



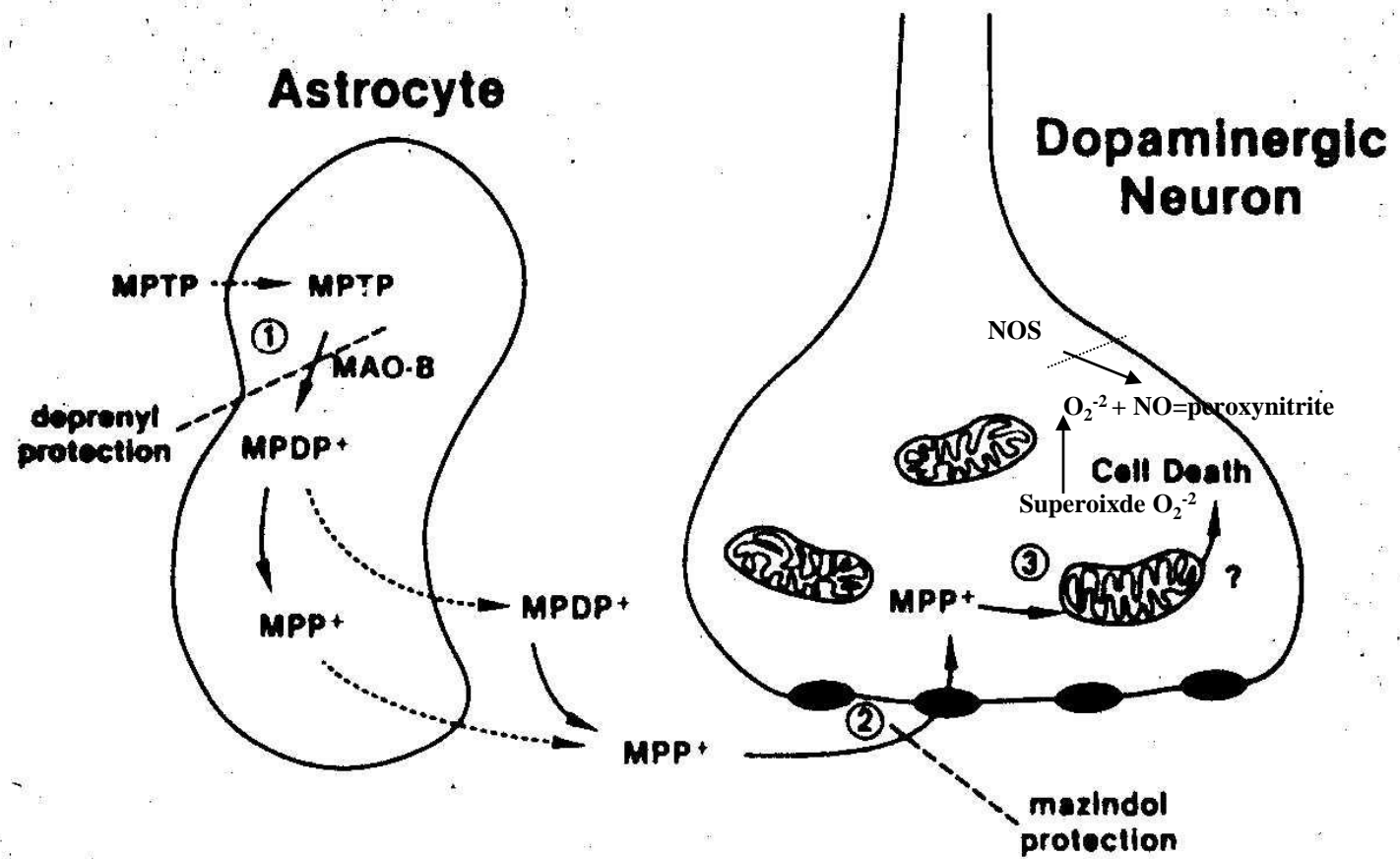


FIGURE 1. Model depicting the postulated mechanism of action of the nigral neurotoxin MPTP. (From Sonsalla and Golbe.³⁴ Reprinted by permission.)

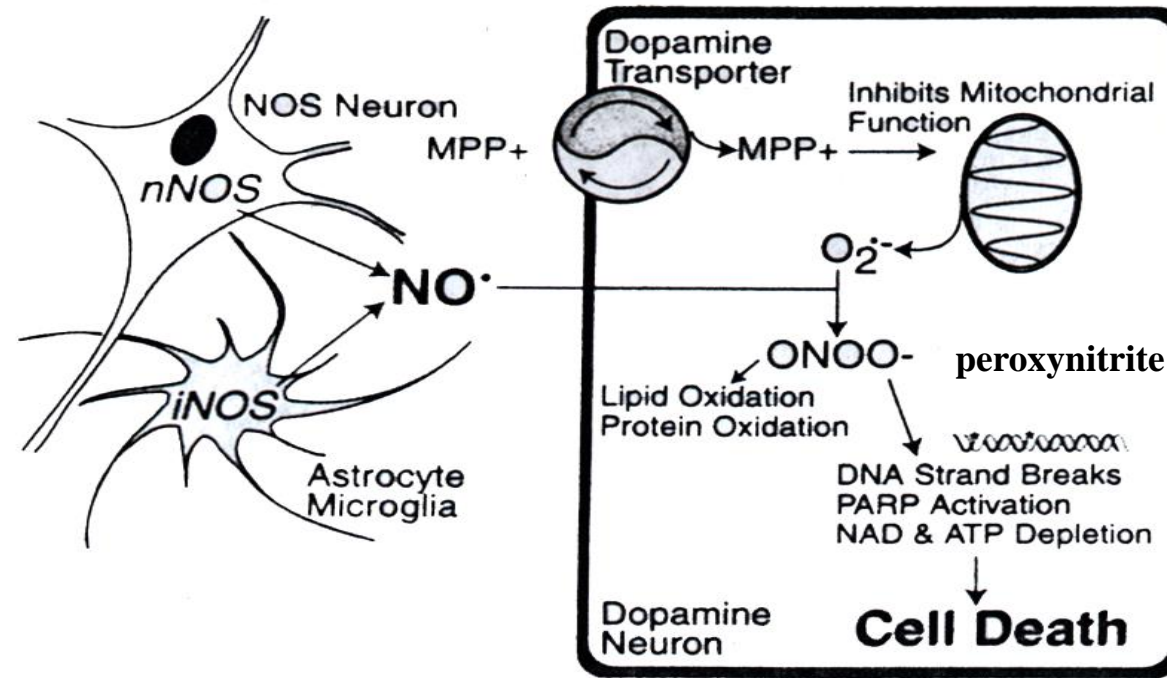
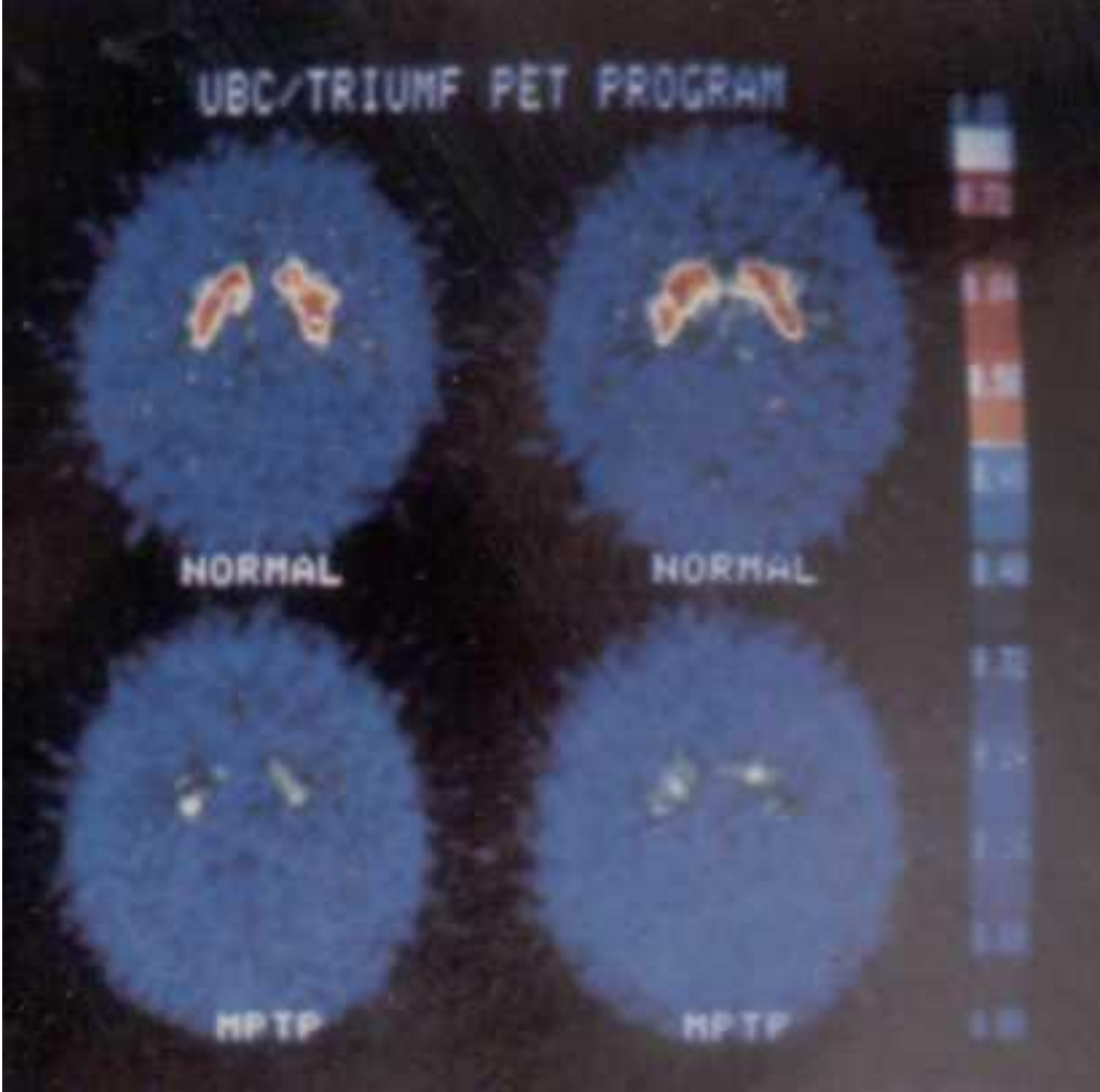


FIG. 1. Model of MPTP-induced dopaminergic cell death. MPP⁺, the active metabolite of MPTP, is concentrated in DA neurons via the high affinity dopamine transporter. MPP⁺ is then concentrated in mitochondria where it inhibits complex 1, which leads to superoxide anion (O₂⁻) formation. The superoxide anion reacts with nitric oxide (NO) which is produced by both neuronal NOS (nNOS) and inducible NOS (iNOS) to form peroxynitrite (ONOO⁻), which damages intracellular proteins and DNA to cause cell death. DNA damage activates the poly (ADP-ribose) polymerase (PARP), which depletes cells of energy stores through decrements in NAD and ATP. This coupled with mitochondrial poisoning leads to cell death. This model may have direct relevance to idiopathic PD as postmortem analysis reveals increases in nitrotyrosine, a marker of ONOO⁻ mediated damage, and induction of iNOS.

**Human BG
18-Fluoro-DOPA
PET scan**

**Parkinsonian
-like individuals**

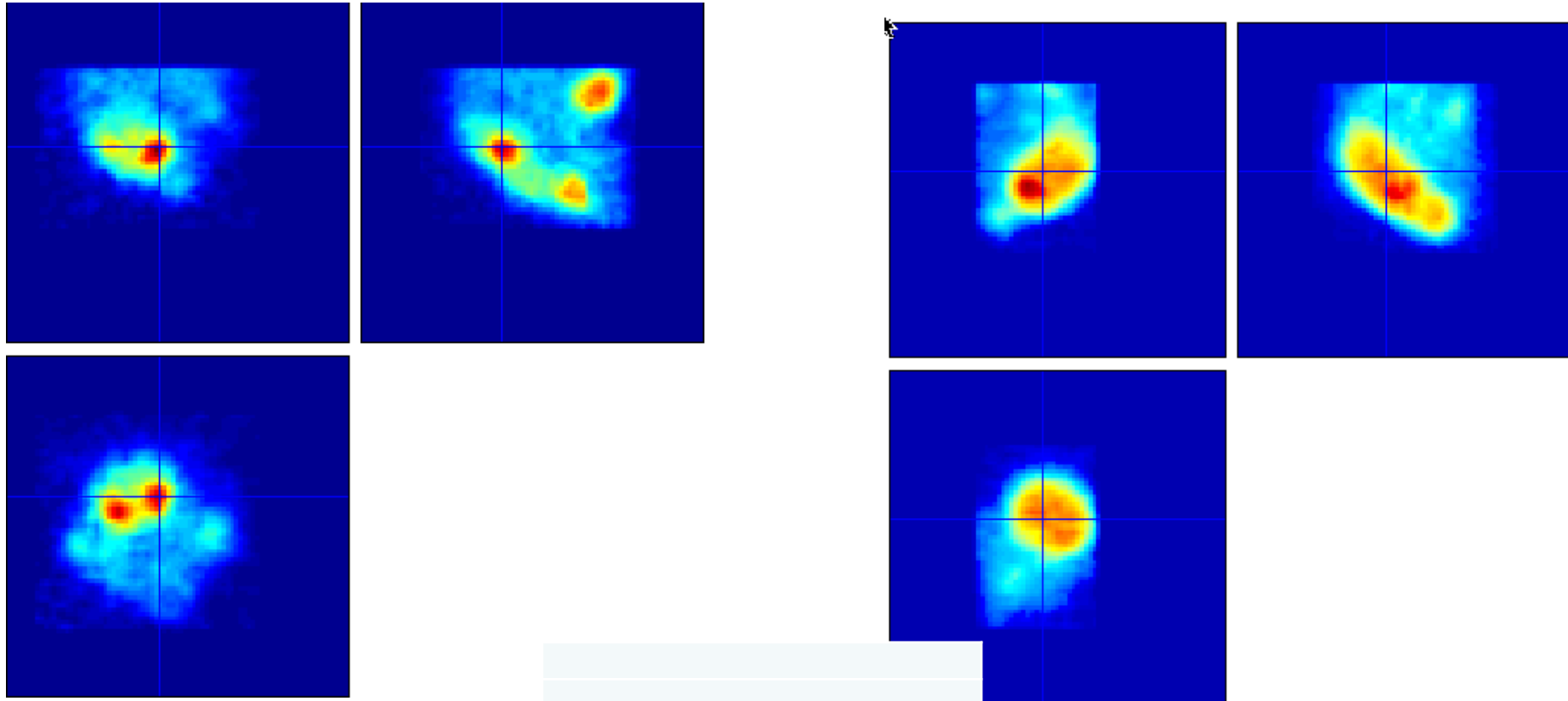


Environmental toxins – pesticide and fungicide cause loss of DA terminals in striatum.

PET – Mouse 11C- methylphenidate (binds to DAT)

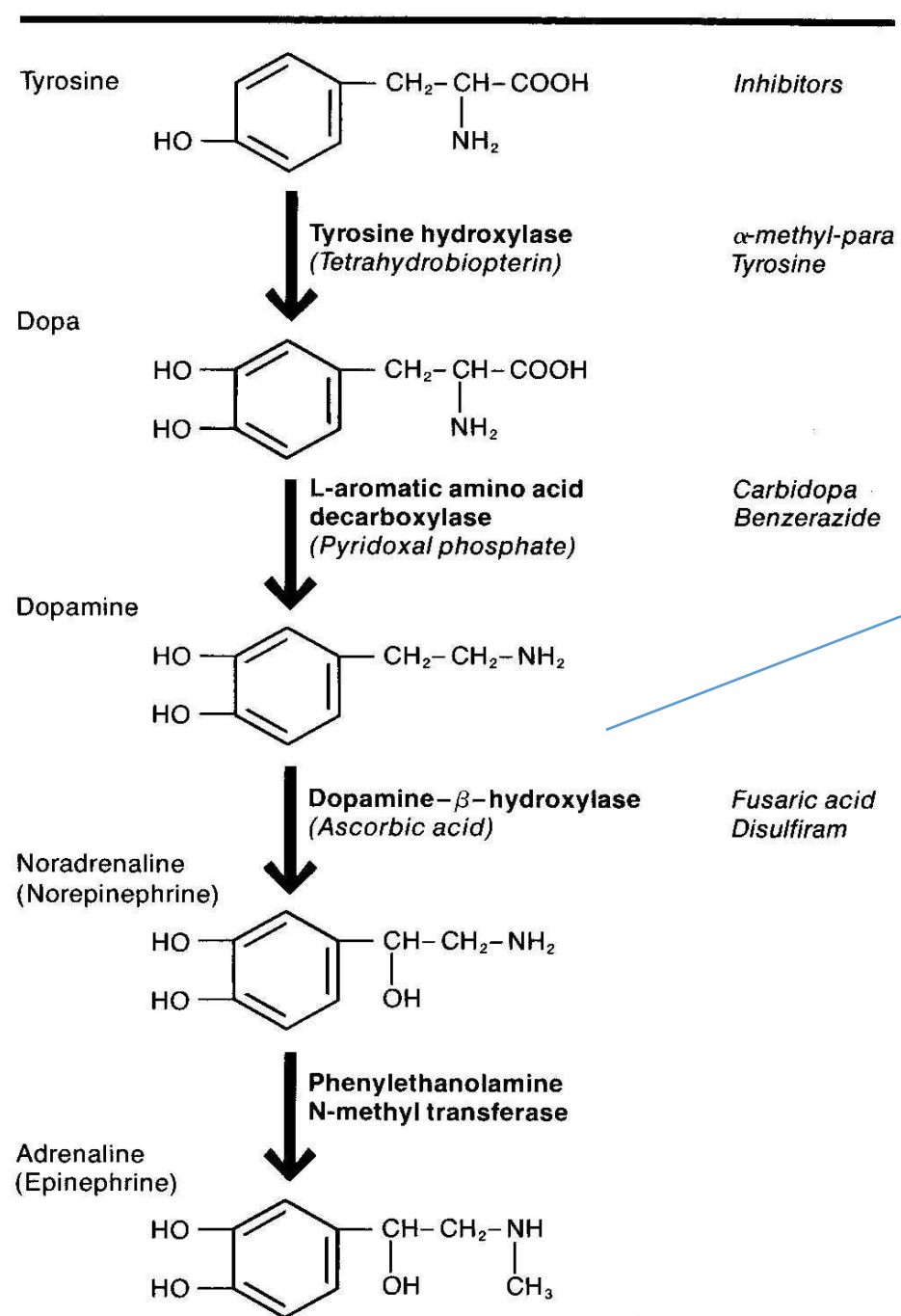
Control

Paraquat + Maneb



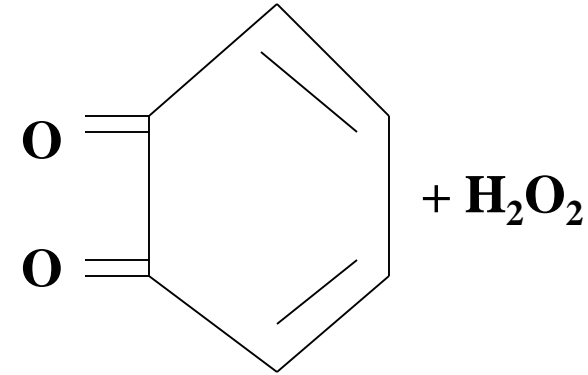
	Mean \pm SEM	
Baseline	1.1183 \pm .09228	
Saline	1.2150 \pm .00500	
PQ/M	.6967 \pm .03180	

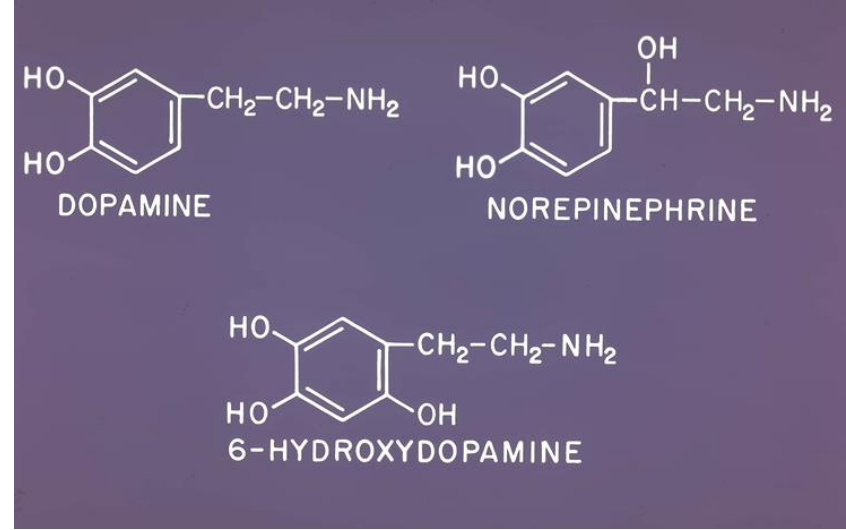
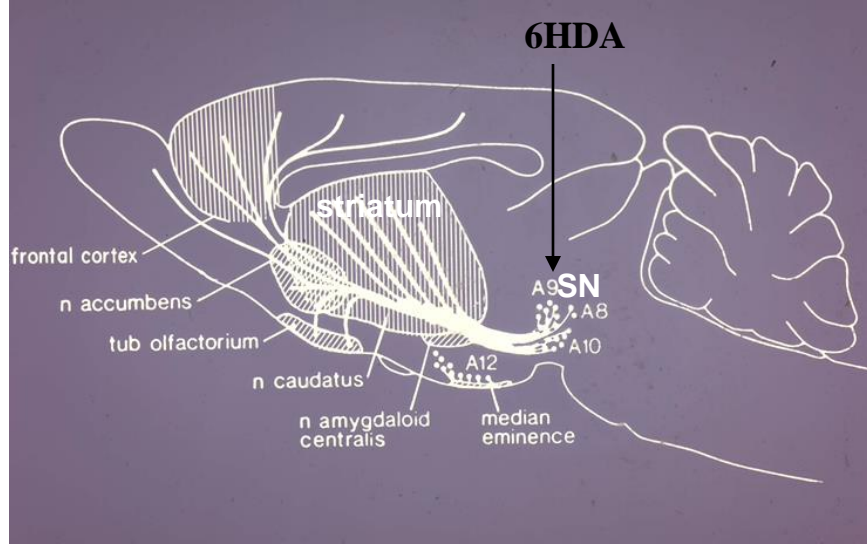
Figure 2-6. Synthesis of catecholamines.



Dopamine Toxicity Hypothesis

Potential toxic metabolites:





Loss of Tyrosine Hydroxylase staining in striatum (caudate) after 6HDA

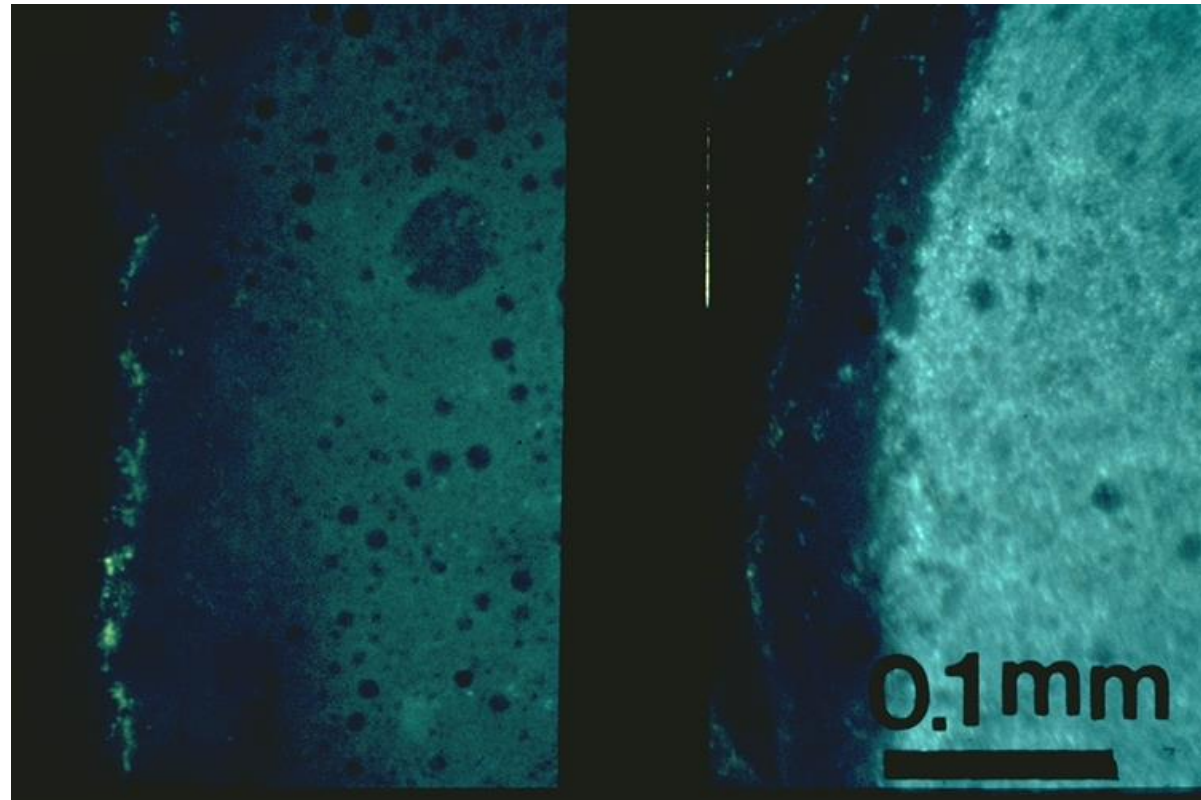
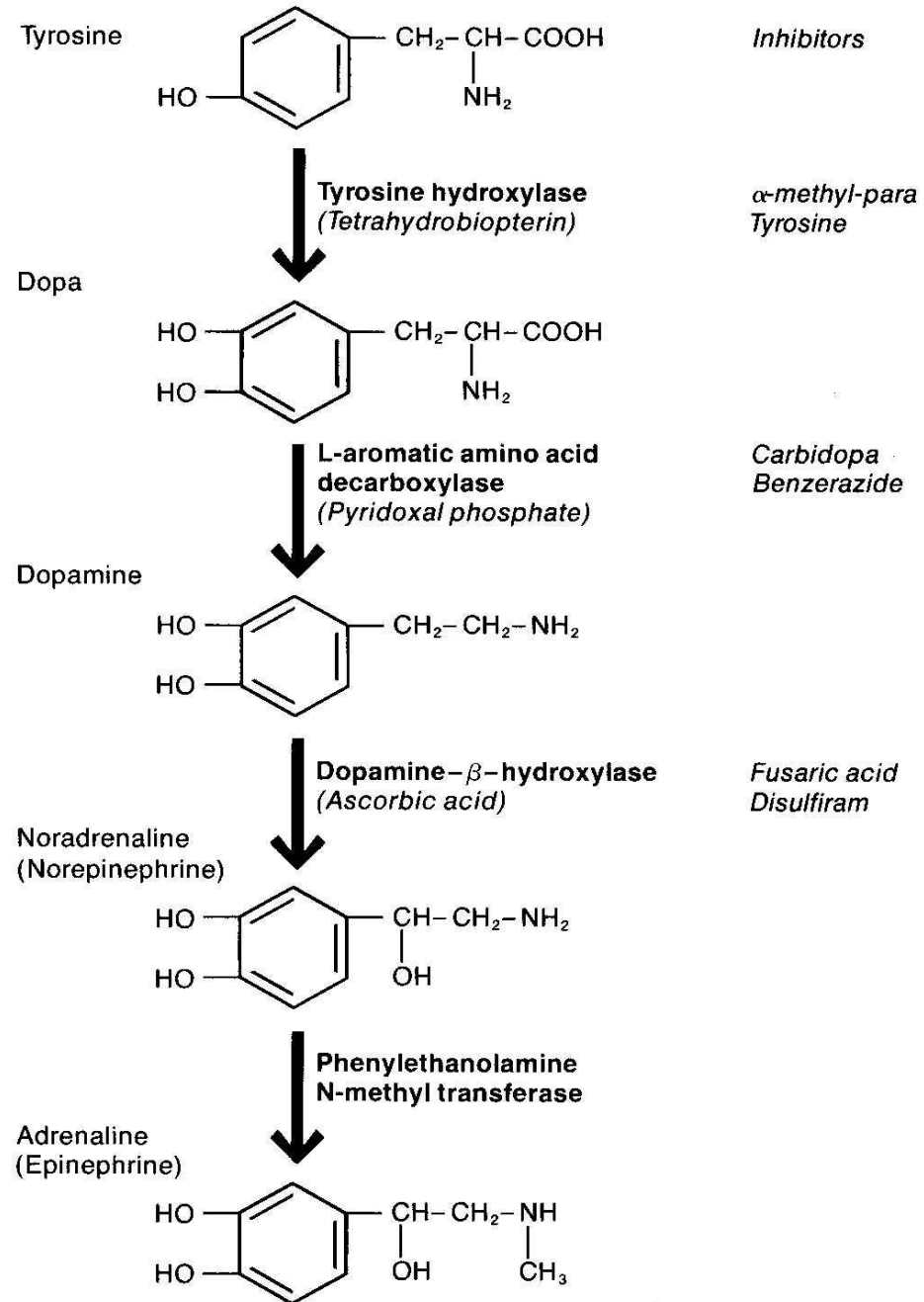


Figure 2-6. Synthesis of catecholamines.



L-DOPA Therapy (Oleg Hornykiewicz) ←

Dyskinesia after I-DOPA movie

<https://www.youtube.com/watch?v=4S56JGo826g>

<https://www.youtube.com/watch?v=EckPVTZIfP8>

Dyskinesia induced by levodopa in parkinson - YouTube

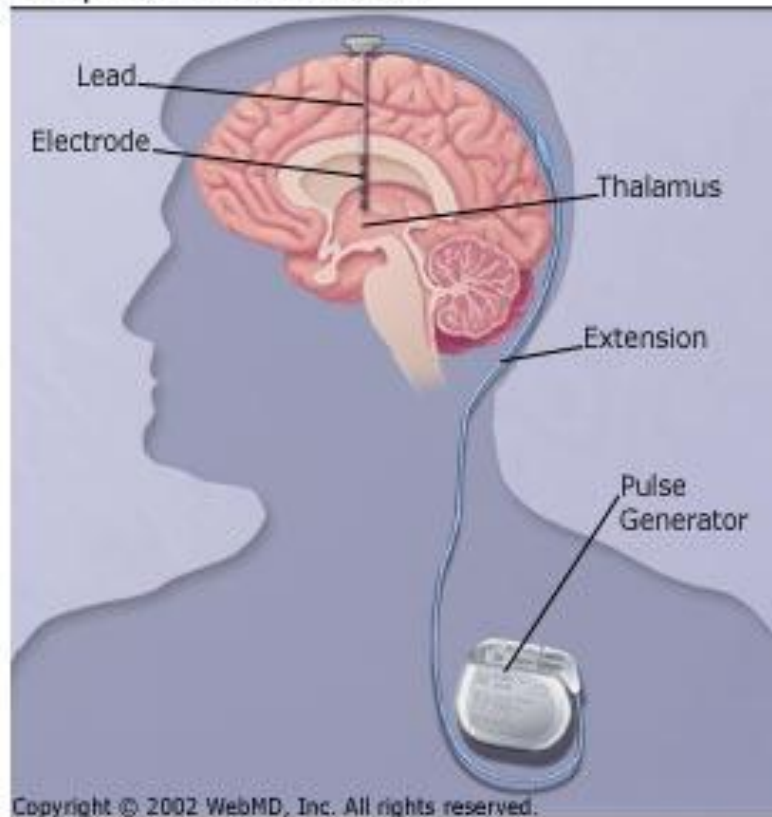
Video for levodopa dyskinesia video ▶ 0:33

<https://www.youtube.com/watch?v=knZQ6iYN4uc>

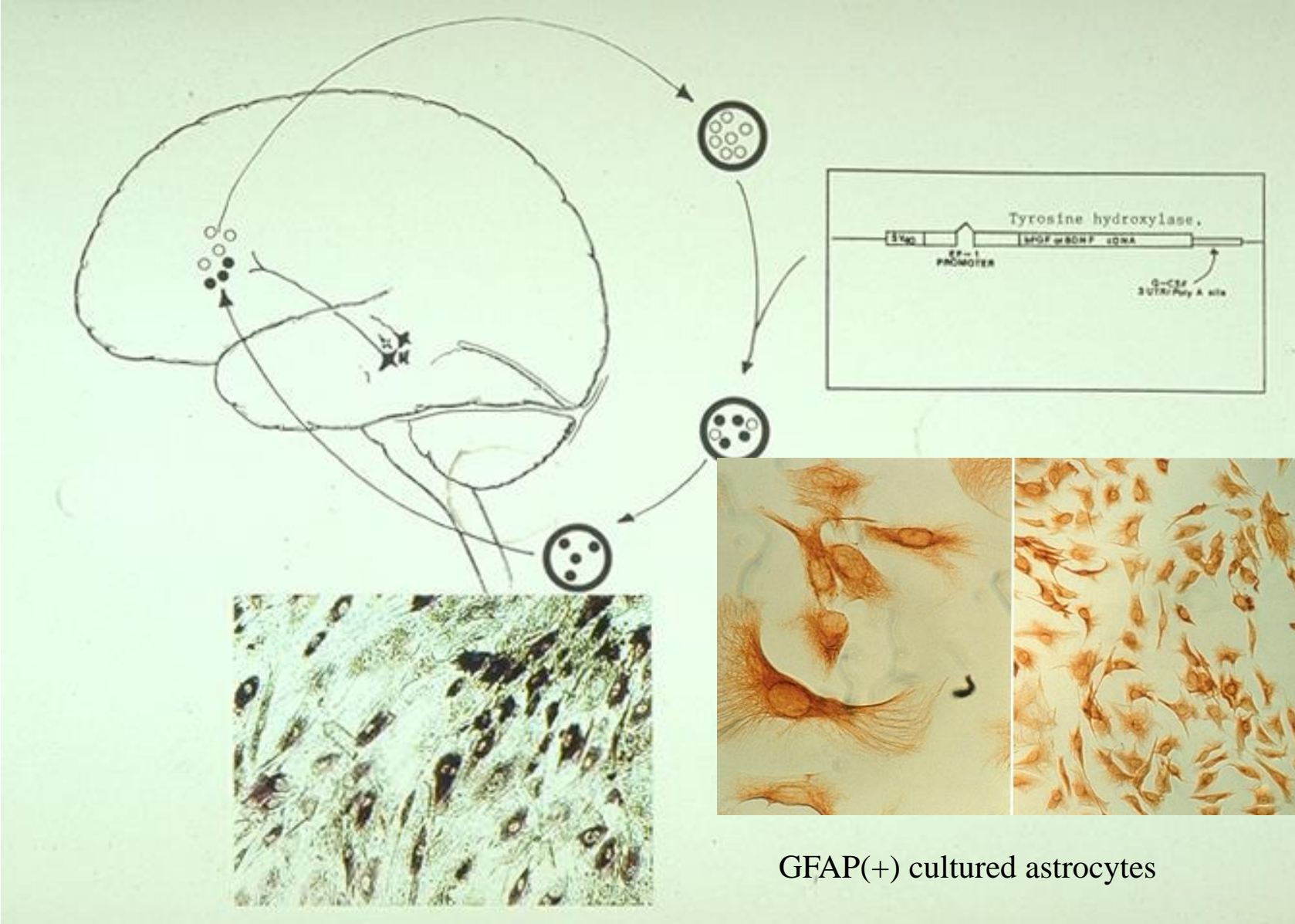
Jun 6, 2017 - Uploaded by Rimon Haque

Your browser does not currently recognize any of the video formats available. Click here to visit our frequently ...

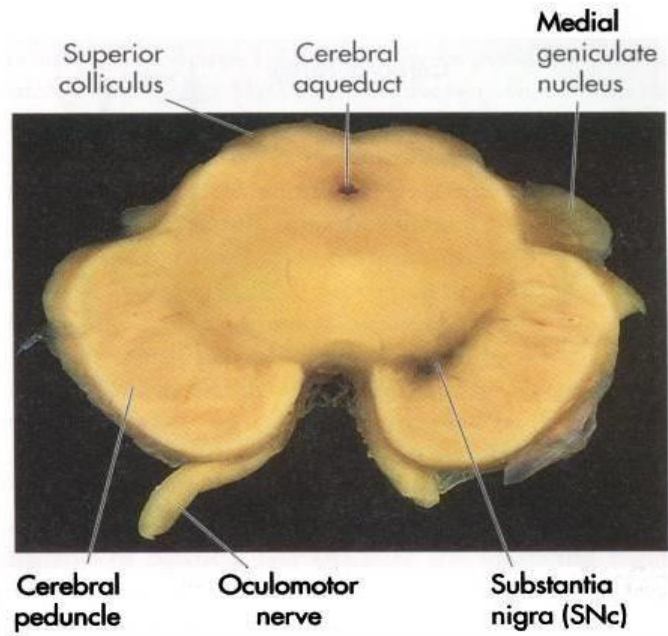
Deep Brain Stimulation



Ex vivo gene therapy - autologous transplants



unilateral PD



Diseased site

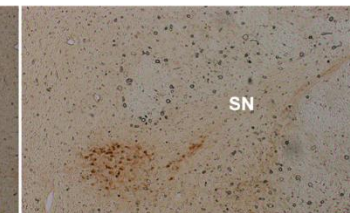
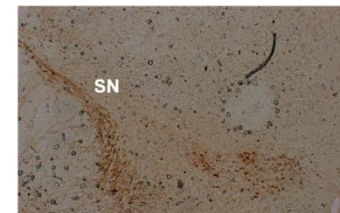
Unilateral lesions with 6hDA in mice

contralateral ipsilateral (6HDA)

striatum



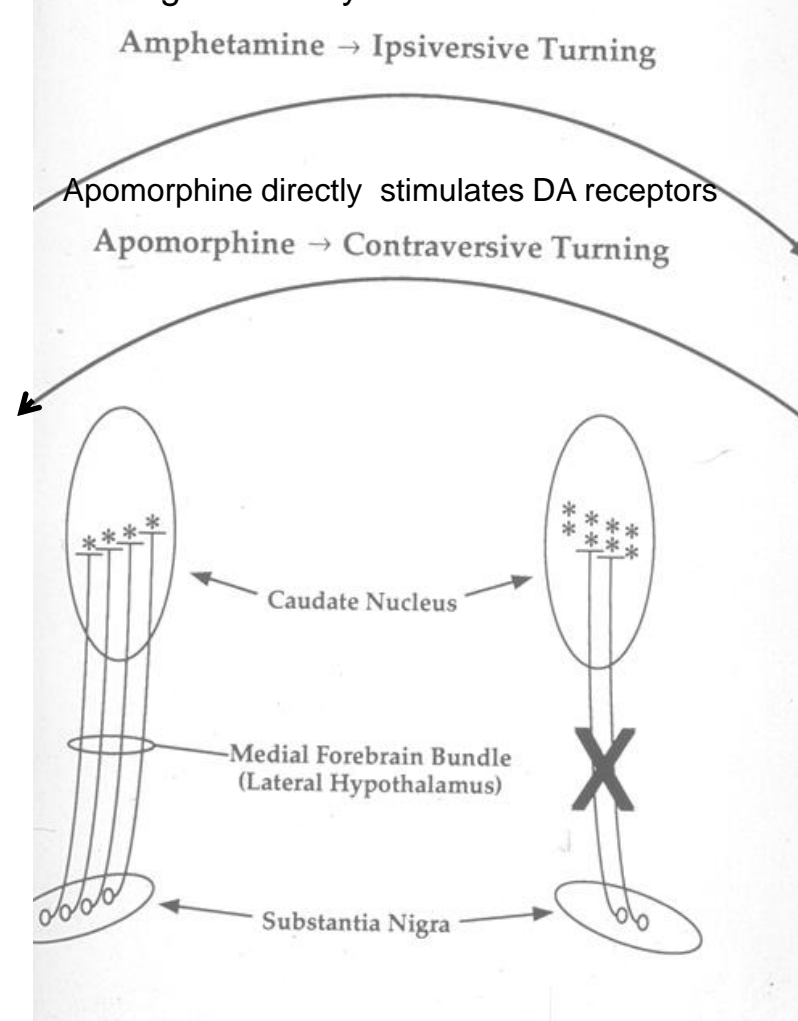
Substantia Nigra (SN)



(TH immunostaining)

Unilateral lesions of DA neurons causing asymmetric motor activity

Spontaneous ipsiversive turning caused by relative excess of DA on nonlesioned side



Neurons derived from reprogrammed fibroblasts functionally integrate into the fetal brain and improve symptoms of rats with Parkinson's disease

[Marius Wernig](#) ^{*},

[Jian-Ping Zhao](#) [†],

[Jan Pruszak](#) [‡],

[Eva Hedlund](#) [‡],

[Dongdong Fu](#) ^{*},

[Frank Soldner](#) ^{*},

[Vania Broccoli](#) [§],

[Martha Constantine-Paton](#) [†],

[Ole Isacson](#) [‡], and

[Rudolf Jaenisch](#)

Modeling neurodevelopment

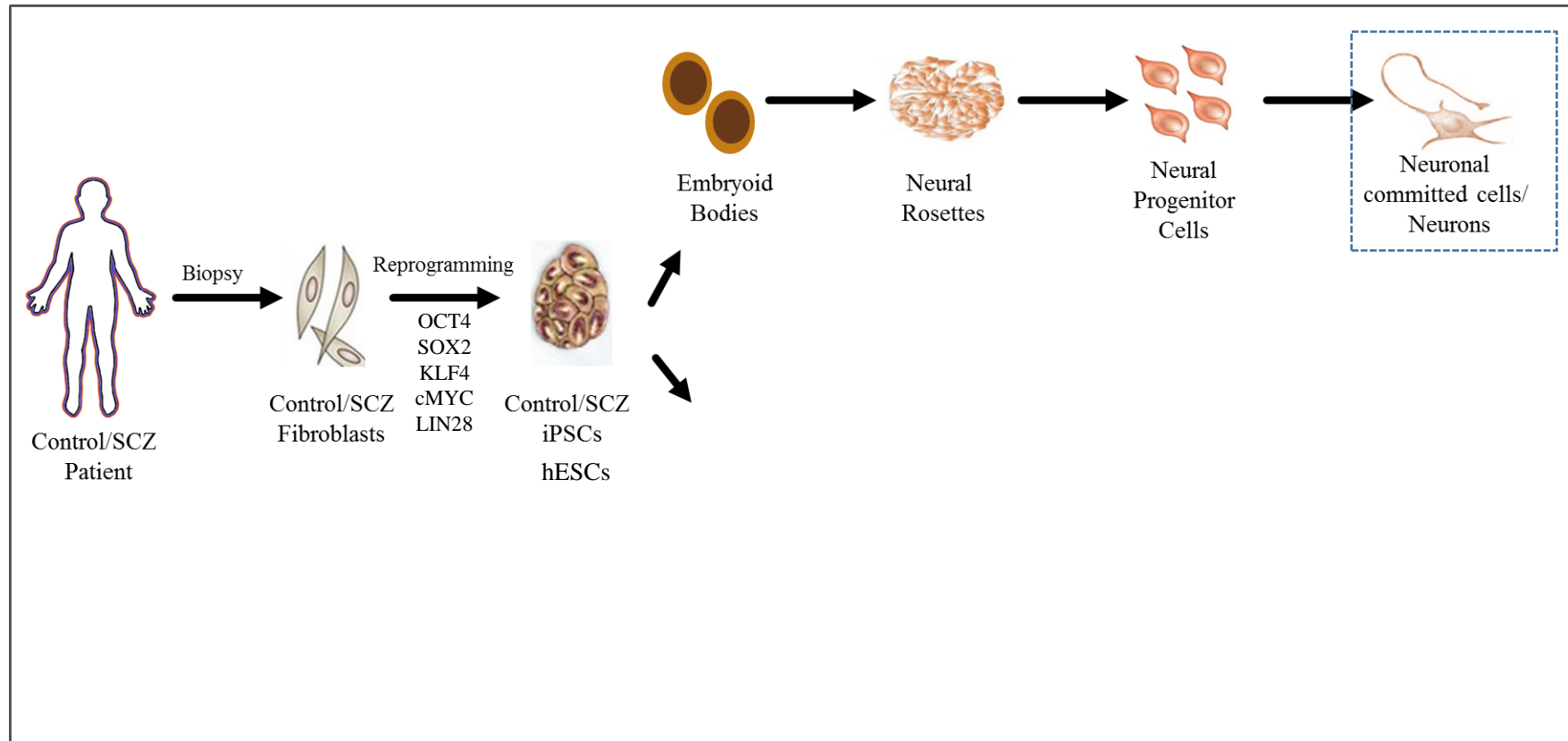
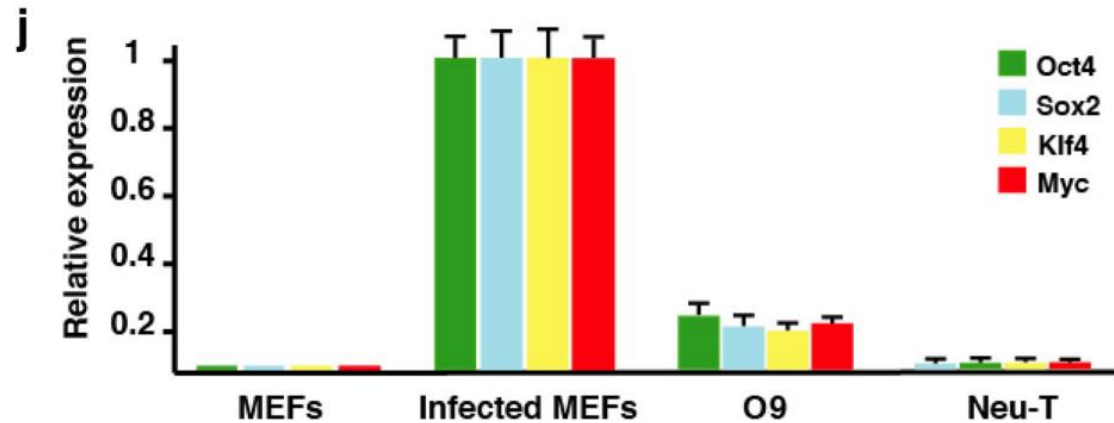
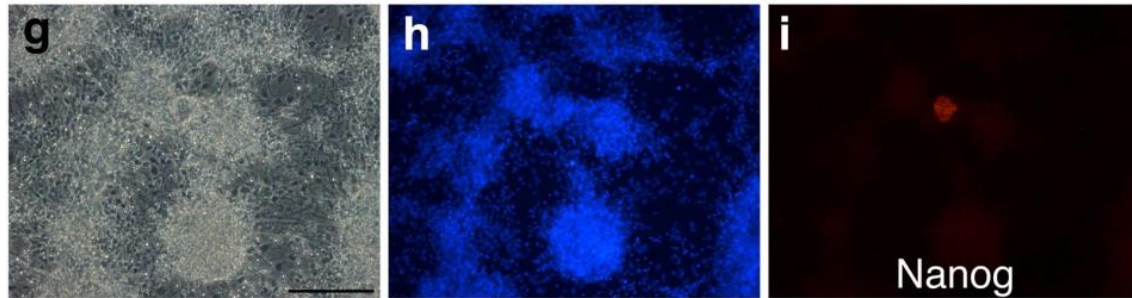


Fig. S3.

(g) Presence of undifferentiated iPS cell colonies in neuronal cultures over 3 weeks after the induction of differentiation. **(h)** Corresponding DAPI staining. **(i)** Undifferentiated colonies are immunoreactive with Nanog antibodies (red). **(j)** Relative expression levels of viral transcripts using quantitative PCR analysis in uninfected MEFs (MEFs), MEFs two days after infection with the four viruses, the Oct4-neo selected iPS cell line O9, and in a teratoma (Neu-T), which had formed 4 weeks after transplantation of unsorted, differentiated iPS cells enriched for dopamine neurons. [Scale bars: 500 μ m (*b*), 50 μ m (*c-f*), 100 μ m (*g-i*).]



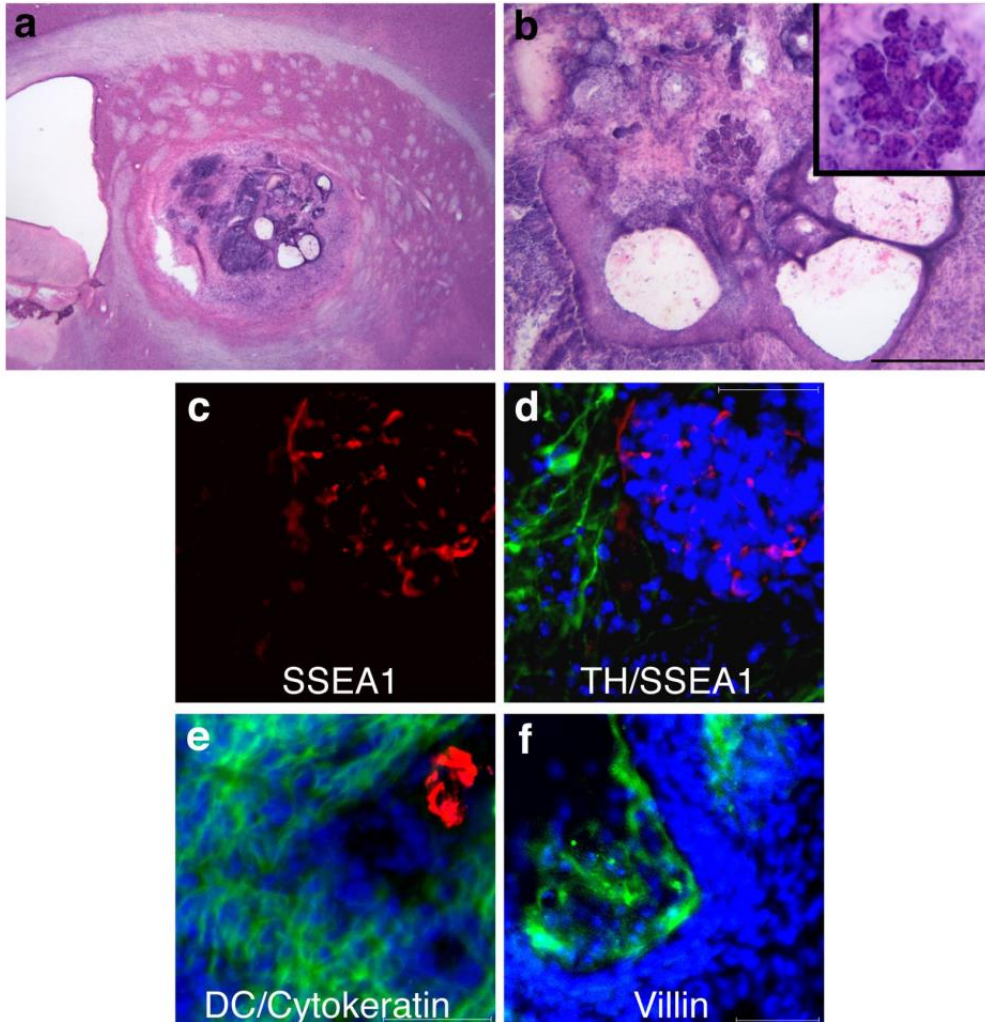


Fig. S3. Teratoma formation after transplantation of iPSC. (a) Overview of one H&E-stained section of a graft, which partly consists of a tumor showing signs of nonneural differentiation indicating the formation of a mature teratoma. (b) Higher magnification of the same tumor showing **squameous epithelium and salivary gland** structures (*Inset*). (c and d) Groups of cells in the teratoma are immunoreactive with antibodies against SSEA1 (red, (**stage-specific embryonic antigen-1**)-) adjacent to neurons expressing TH (green). The blue color represents DAPI staining. (e) The tumors contain epithelial cells which express cytokeratin (red) and doublecortin (DC)-positive cells (green). (f) Other cellular structures are villin-positive (green).

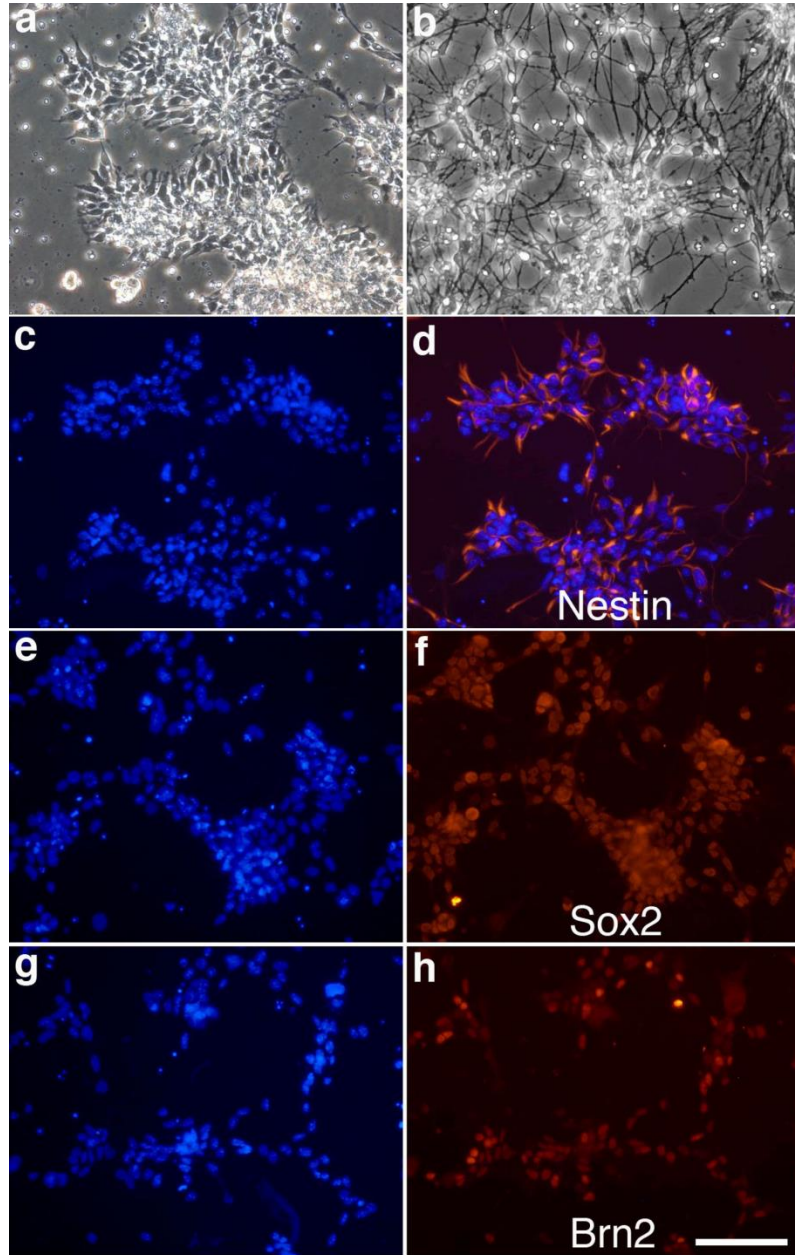


Fig. S1. Characterization of iPS cell-derived neural precursor cells. (a) iPS cell-derived neural precursor cells growing in FGF2-containing media show a cell morphology characteristic of regular neural precursor cells. (b) Six days after withdrawal of FGF2, the cells adopt a more differentiated morphology. (c–h) The FGF2-responsive cells stain for the neural precursor cell markers Nestin (intermediate filament) (c and d), Sox2 (e and f), and Brn2 (POU homeodomain protein) (g and h). (c, e, and g) DAPI-stained micrographs of the corresponding visual field. (Scale bar: 100 μ m.)

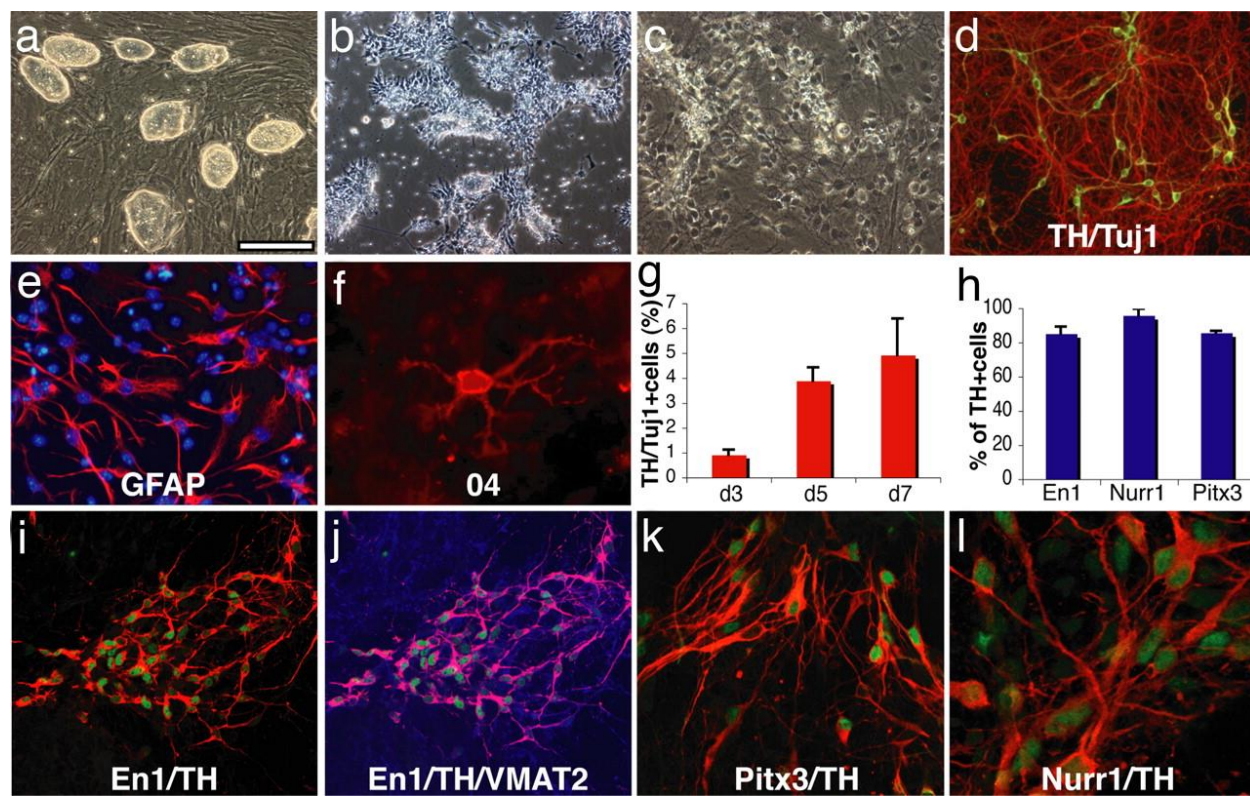


Fig. 1. *In vitro* differentiation of induced pluripotent stem cells. (a) The undifferentiated Oct4-selected iPS cell line O9. (b) FGF2-responsive neural precursor cells. (c) Differentiated neural morphologies 7 days after growth factor withdrawal. (d) A fraction of β -III-tubulin positive neurons (red) are double labeled with antibodies against TH (green, yellow in merged image), 7 days after growth factor withdrawal. (e and f) At this stage, also, many GFAP-positive astrocytes (red) (e) and rare O4-positive oligodendrocytes (f) are found. (g) The fraction of TH-positive cells over β -III-tubulin positive cells increases along neuronal maturation (mean and standard deviation, three independent experiments). (h) The vast majority of TH-immunoreactive cells coexpress En1, Pitx3, and Nurr1 (mean, standard deviation). (i) Coexpression of En1 (green) and TH (red). (j) **VMAT2** (vesicular monoamine transporter 2) and TH [purple in the merged image indicates colocalization of TH (red) and VMAT2 (blue)]. (k and l) Most TH-positive cells (red) are also positive for Pitx3 (green) (k), and Nurr1 (green) (l) after 7 days of neuronal differentiation. [Scale bar in a: 200 μ m (a and b), 100 μ m (c, d, i, and j), 50 μ m (e and k), and 20 μ m (f and l).]

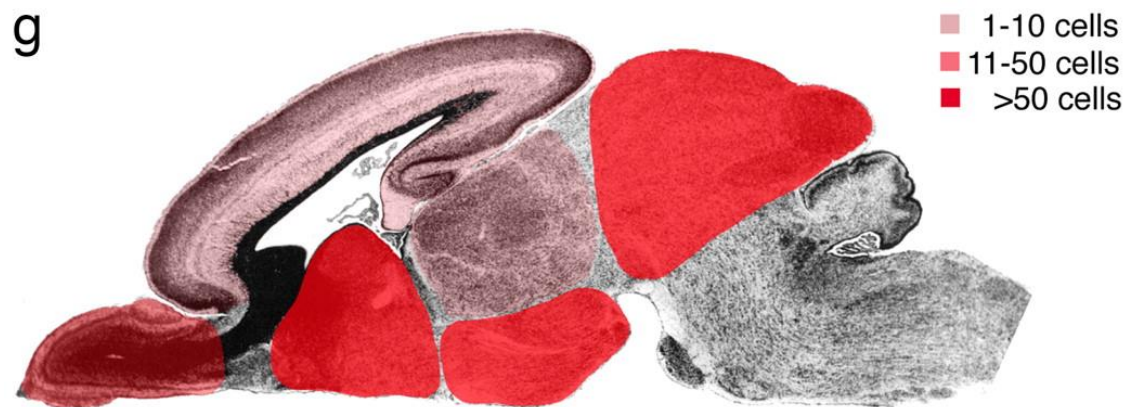
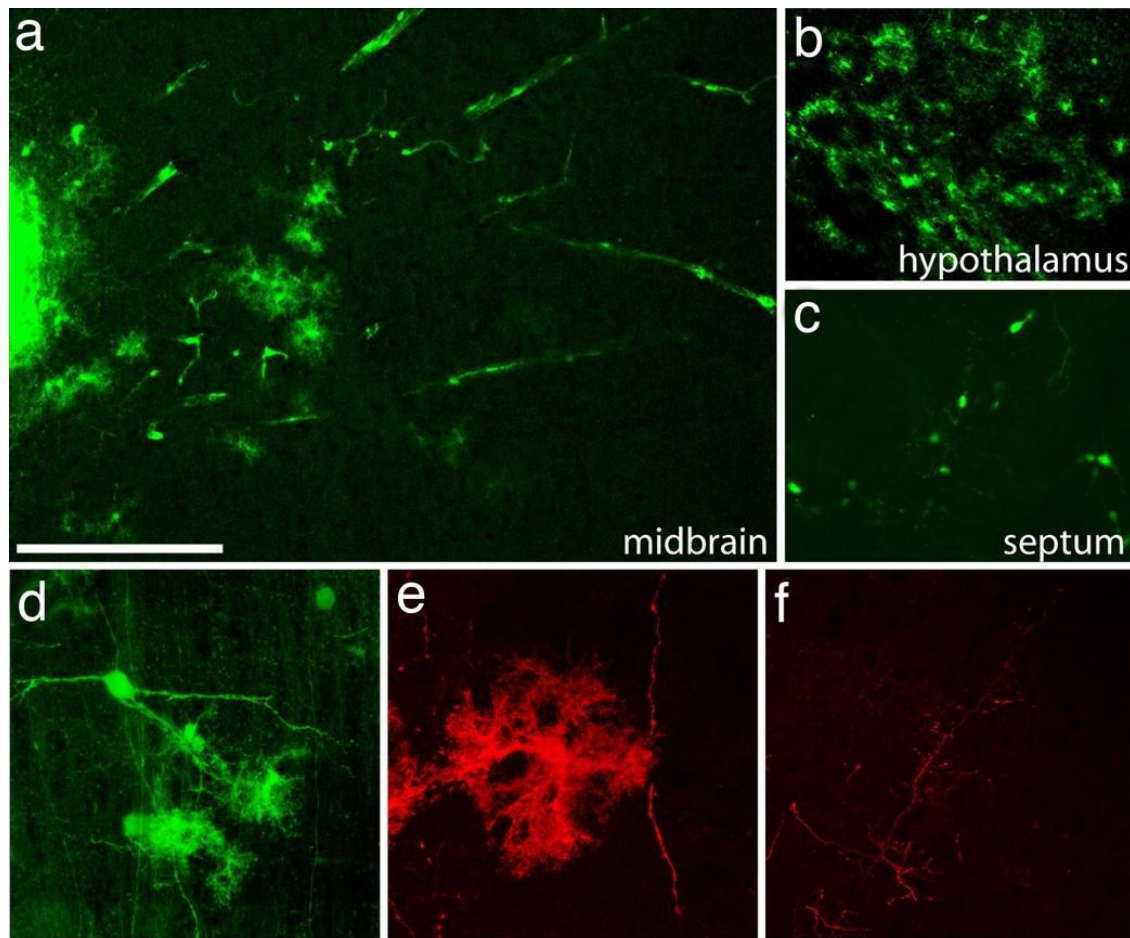


Fig. 2. Extensive migration and differentiation of iPS cell-derived neural precursor cells in the embryonic brain. (a) Transplanted cells form an intraventricular cluster (left part of the image) and migrate extensively into the tectum 4 weeks after transplantation into the lateral brain ventricles of E13.5 mouse embryos. (b) A high density of integrated astrocyte-like cells in the hypothalamus. (c) Complex neuronal morphologies of GFP-positive cells in the septum. (d) Confocal reconstruction of grafted GFP-fluorescent cells in the tectum with neuronal and glial morphologies. (e) GFP immunofluorescence and confocal reconstruction identifies an astrocytic cell and a long neuronal process. (f) Similarly, GFP-immunoreactive, fine neuronal processes are crisply delineated. (g) Schematic representation of the main integration sites of iPS cell-derived neurons and glia. Color codes represent different ranges of cell numbers. Shown are the highest incorporation density across all analyzed brains. See [Table 1](#) for more details. [Scale bar in *a*: 200 μm (*a-c*), 100 μm (*d* and *f*), and 50 μm (*e*).]

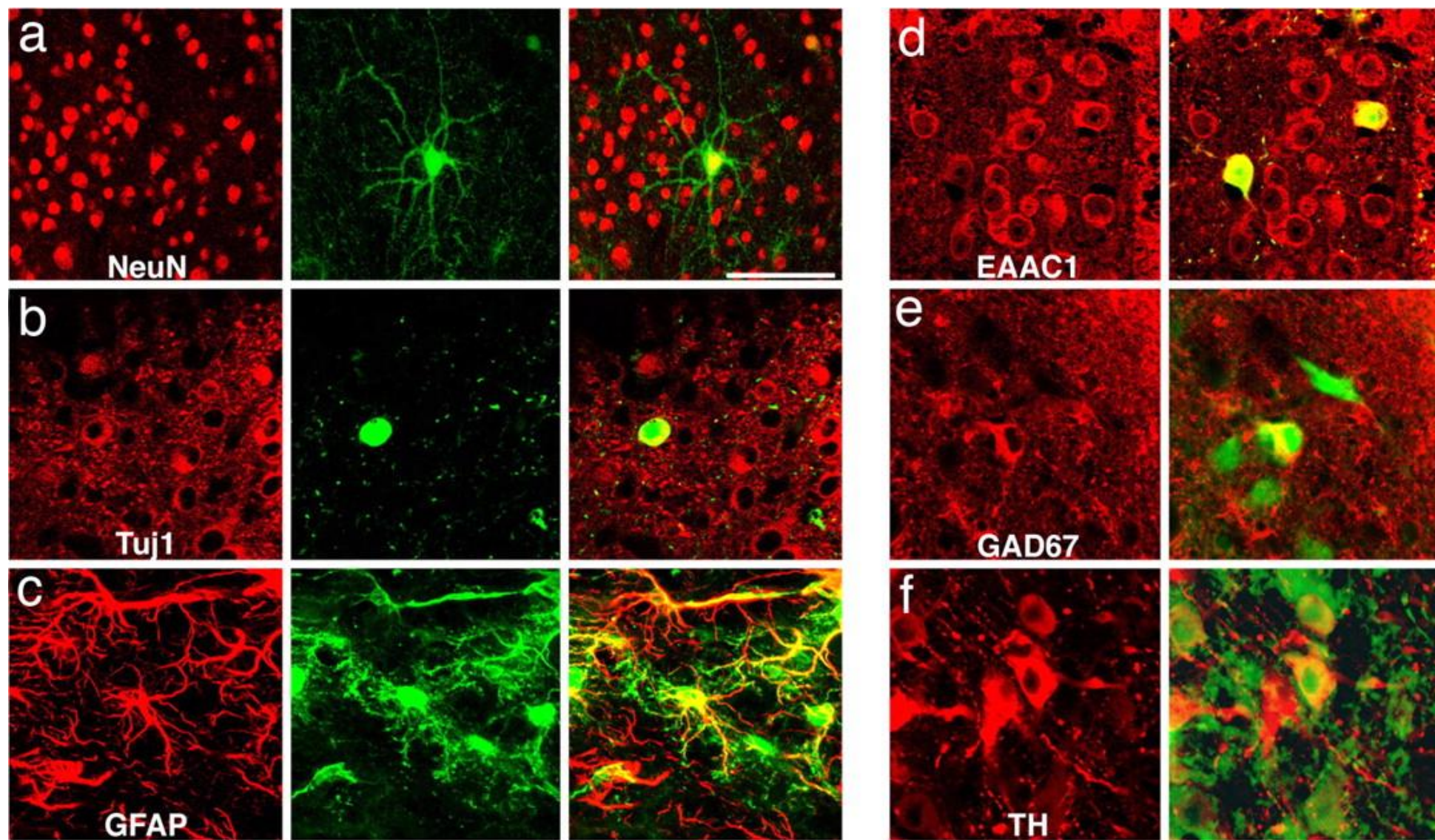


Fig. 3. Embryo-Transplanted cells express neuronal and glial markers. (a) Confocal reconstruction of a GFP-positive cell in the midbrain (green) expressing NeuN (red) 4 weeks after intrauterine transplantation. (b) Another transplanted neuron (green) expresses cytoplasmic β -III-tubulin (red) as shown in this confocal section. (c) Other cells can be colabeled with GFAP antibodies (red). (d) Both host neurons (red only) and transplanted cells (yellow) express the glutamate transporter EAAC1. (e) Soma of grafted cells (green) can be labeled with antibodies against GAD67 (red). (f) TH-immunoreactivity (red) can be found in both host and grafted neurons (green). [Scale bar in *a*: 100 μ m (*a-c*) and 50 μ m (*d-f*).]

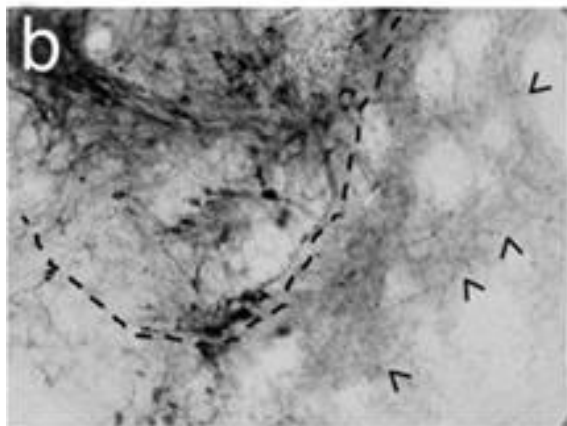
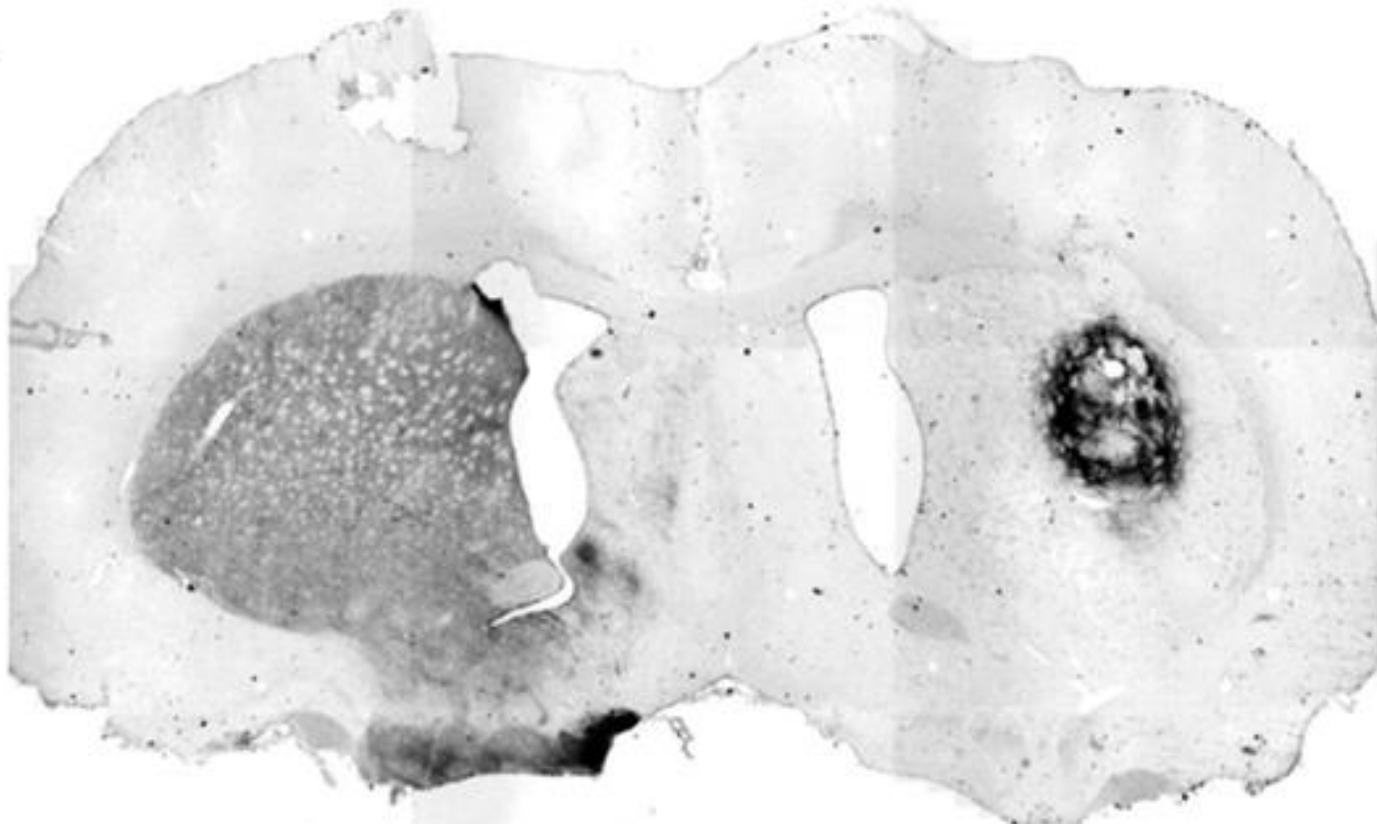
a

Fig. 5. iPS cell-derived neurons integrate into the striatum of hemi-parkinsonian rats and improve behavioral deficits. (a) Overview of an iPS cell graft 4 weeks after transplantation stained with antibodies against TH (dark brown). **(b)** Higher magnification of another graft showing TH-positive soma and the dense innervation of the surrounding host striatum by donor-derived neurites (arrowheads). The dashed line indicates the edges of the graft. (

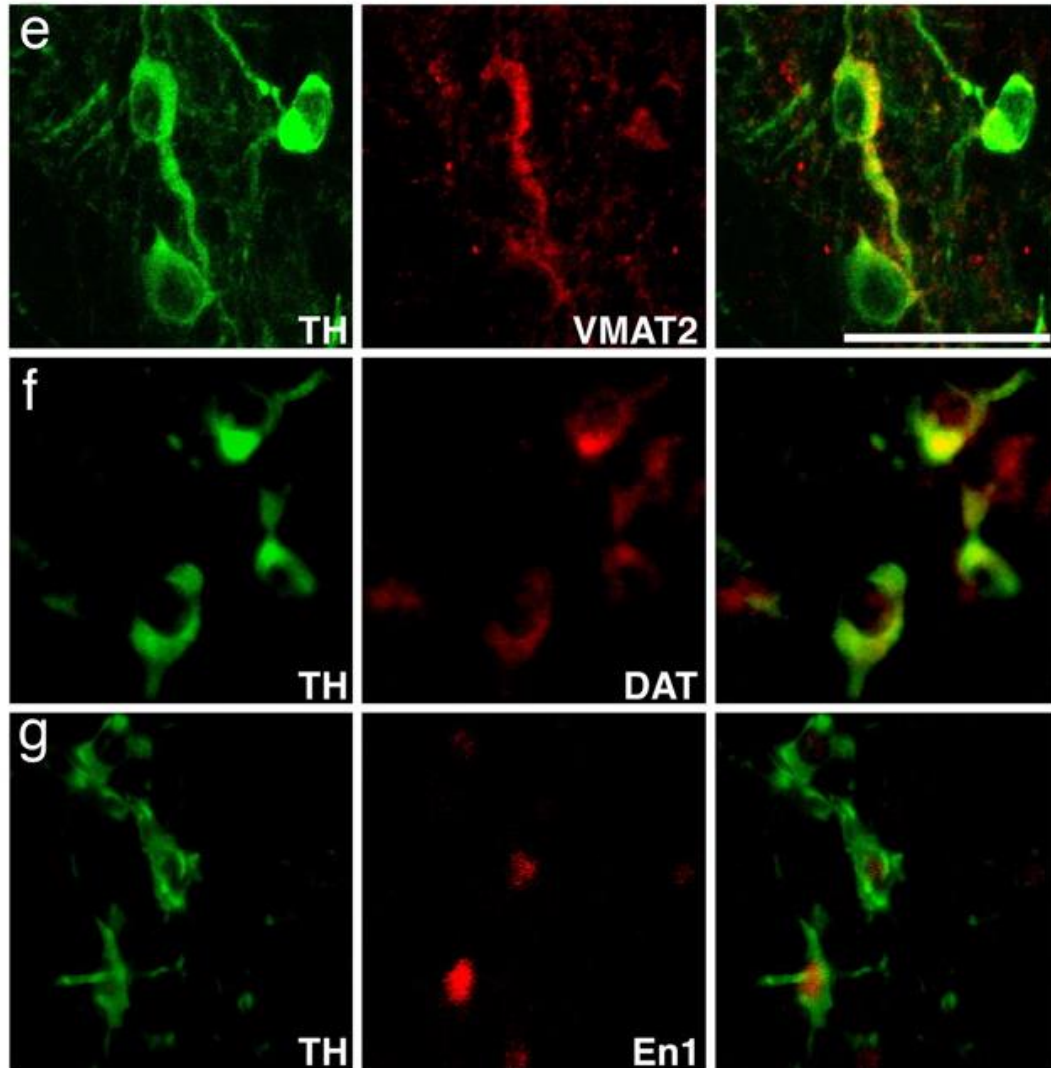


Fig. 5. iPS cell-derived neurons integrate into the striatum of hemiparkinsonian rats (*e–g*) The grafted TH-positive cells (green) can be colabeled (red) with antibodies against VMAT2 (*e*), DAT (*f*), and En1 (*g*). (Scale bar: 50 μ m.)

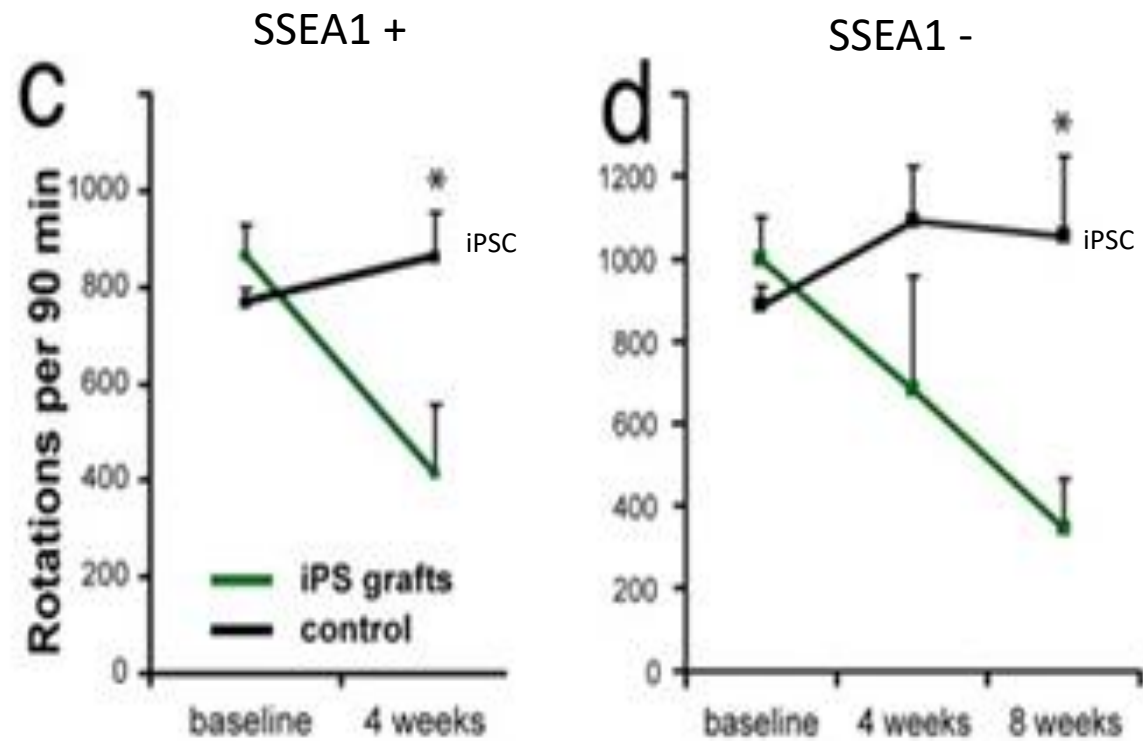


Fig. 5. iPS cell-derived neurons integrate into the striatum of hemi-parkinsonian rats and improve behavioral deficits.. (c) Amphetamine-induced rotations are significantly reduced in animals grafted with unsorted iPS cell populations (green, $n = 5$) compared with the sham control animals (black, $n = 10$) ($P = 0.0185$, unpaired Student's t test). Shown are the number of rotations in 90 min after amphetamine injection as means and standard deviations. (d) Amphetamine-induced rotations in animals transplanted with iPS cell cultures after elimination of SSEA1 (**stage-specific embryonic antigen-1**)-positive cells by FACS. Grafted animals (green, $n = 4$) show significant recovery compared with control animals (black, $n = 10$) ($P = 0.006$).